Geo-information Science and Remote Sensing

Thesis Report GIRS-2018-26

Improving tree crown identification

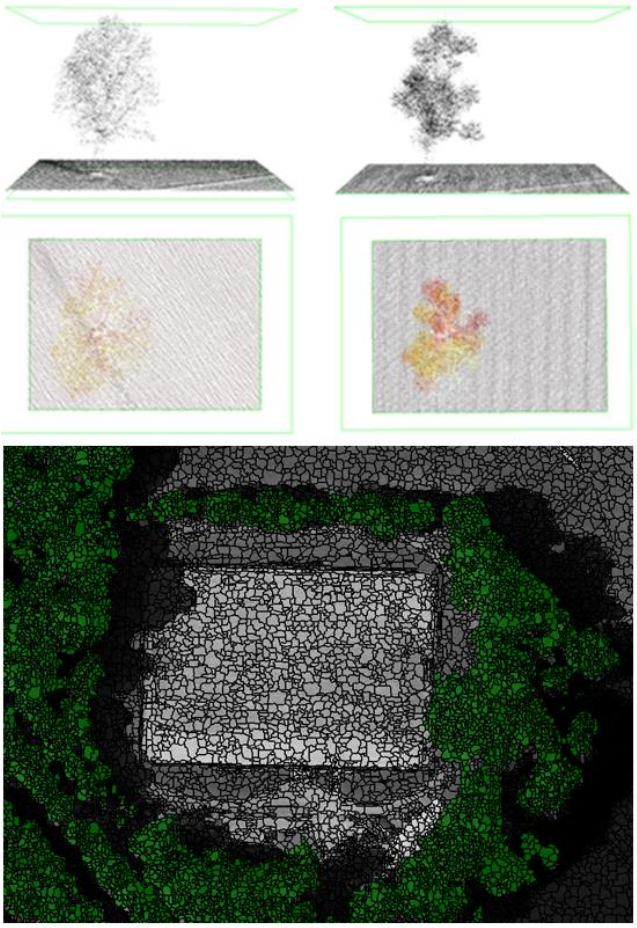

18-05-2018

WAGENINGEN
UNIVERSITY & RESEARCH

Improving tree crown identification

Master Thesis

Author:
Stijn Wijdeven
Master Geo-Information Science
Wageningen University & Research

Supervisors:
Ron van Lammeren
Frans Rip

Date & Location:
March 22nd, 2018, Nijmegen

Abstract

There is need for a standardized method for automated tree crown identification. In this study, two methods are analysed to identify their best practices and to develop a new, hybrid method. Method one is based on a Digital Surface Model (DSM), which determines the presence of trees based on their height compared to their neighbouring pixels. Method two is based on Object-Based Image Analysis (OBIA), which determines the presence of trees based on pixel characteristics of high resolution aerial images. Based on the best practices of both methods the hybrid method is created with the aim to improve tree crown identification accuracy. The results of the DSM-, OBIA- and hybrid methods are compared to a validation dataset by their correct number of crowns counted and crown area size. This is done for single solitary trees, for trees standing in rows and for trees as part of a group. For identifying individual tree crowns, the results show that single trees are more easily identified than trees in rows and groups. Furthermore, the performances of both the DSM-method and OBIA-method increase when using input data of a higher resolution. Based on the results it is not possible to conclude that the hybrid method is an overall improvement compared to the DSM- and OBIA-methods. Rather, it depends on what somebody wants to achieve with the crown identification method to determine what method is most suitable. The hybrid method has proven to be generally more useful for crown area estimation, but is relatively less accurate for crown count estimation.

Key words: *Tree crown identification, crown delineation, Digital Surface Models, DSM, Airborne Laser Scanning, LiDAR, OBIA, Object-Based Image Analysis, Remote Sensing, pointclouds, Boomregister, AHN.*

Table of Contents

Table of Figures

Table of Tables

1. Introduction

Trees have many beneficial properties that improve the liveability for humans. They are vital for air quality and public health, provide shade and coolness in hot urban areas and are a resource of food and shelter for many animals. This makes trees very valuable, however the presence of a tree can also be a nuisance. Roots damage underground cables and pipes, roads and railways may be obstructed by falling branches and diseased trees could harm their environment (Van Herzele & Wiedemann, 2003). The management of trees has to be done carefully to weigh the benefits and risks, making sure that no trees constitute dangerous situations, or are chopped down unnecessarily. Reliable and up-to-date information on the shape, size and species of a tree will help decision making, reducing mistakes in tree management and ultimately improving liveability.

In the Netherlands, each municipality or other land owning governmental agency is responsible for their own public tree management and there is no universally adopted method in place to identify the presence of trees (Verhaar, 2016). Currently, most green space managers are working with maps on which a point represents a tree, however planning based on point data is insufficient for a lot of applications (Verhaar, 2016). Furthermore, because each governmental agency has different priorities, the reliability of the mapped tree data has a countrywide variation. One example is the database of the Dutch tree safety inspection which is managed locally and has variations in periodicity and completeness (Meijer et al., 2015, p. 12).

To meet the need for an automated and consistent method, there have been several attempts to map the countrywide presence of individual trees in the Netherlands. The first method, developed by Alterra Wageningen UR (Meijer et al., 2015), is based on the 'Actueel Hoogtebestand Nederland' (AHN) and uses a Digital Surface Model (DSM) acquired by Airborne Laser Scanning (ALS). A second method uses data acquired from high resolution aerial photographs and is developed by Dutch geo-ICT company NEO. This method uses an object-oriented algorithm to identify and distinguish different tree crowns. A partnership of Alterra, NEO, Geodan and Cobra has taken initiative to create the Boomregister: a national tree register based on LiDAR data and Aerial imagery.

The Boomregister is offered for sale on different administrative levels and is currently used as a planning tool for governments (Verhagen, 2015). This tree register model does have its shortcomings. Not all trees are identified and if multiple trees are in close proximity, for example in a lane or clump, the multiple tree crowns may be identified as one. These shortcomings are determined by comparing the results of the Boomregister with data from the BGT (Basisregistratie Grootschalige Topografie or Base Registration of Large Scale Topography), which is accepted as true reference. The BGT contains all major physical objects in the Netherlands, however it doesn't require all municipalities to deliver information on individual trees. Individual trees need only be included if desired by the provider of the data, which is usually in urban areas (Van den Brink et al., 2013). Crown area identification is useful for estimating biomass, shade or possible nuisances caused by falling leaves or branches. Furthermore, the crown area is used as a variable to indicate the root system of a tree (Verhagen, 2015). Therefore, reliably monitoring the crown area will help with policy making and improve tree management.

1.1 Background

The presence of green space is valuable for several reasons. Trees give human environments a natural and soothing character, contribute to a pleasant microclimate and improve the quality of life (Meijer et al., 2015, p. 5). *"The amount and quality of green spaces affect citizens' patterns of activities, the modes and frequencies of every day recreation, the way knowledge about the environment is acquired, the opportunities to relax of daily stress"* (Van Herzele & Wiedemann, 2003, p. 124). Furthermore, optimally arranged green infrastructure in cities can reduce urban temperatures and improve air quality. However, tree information inventory, particularly on private properties, is labour intensive and the results are not spatially explicit (Alonzo, Bookhagen & Roberts, 2014).

In the last twenty-five years the possibilities to use digital media for tree inventory have grown, but in practice the use of GIS and remote sensing based solutions are not often used (Nijhuis, 2013, p. 88 - 90). The tree register methods developed by Alterra and NEO are successful in covering a country wide digital tree identification, however they still have limitations when identifying individual tree crowns. The NEO-method uses an Object-Based Image Analysis to identify trees on high resolution aerial images. The digital surface-method developed by Alterra uses height rasters derived from Airborne Laser Scanning (Meijer et al., 2015).

1.1.1 Digital Surface Modelling

Digital Surface Models (DSMs) are a representation of objects on the earth's surface. DSMs are a class of Digital Elevation Models (DEMs), which are usually obtained from remote sensing data (Priestnall et al., 2000). Traditionally, it is possible to construct a DEM by digitising existing topographic maps, using Radar images, or by photogrammetry using stereoscopic aerial photographs (Priestnall et al., 2000). A more recent technique is the use of airborne LiDAR (Light Detection And Ranging) scanning, which is faster and cheaper than photogrammetry or digitising topographic maps and is more accurate than Radar techniques (Leigh et al., 2009). This makes Airborne LiDAR scanning a powerful technique which can be used to acquire reliable elevation surfaces and to classify ground types quickly and efficiently without the need for manipulating multispectral image files (Antonarakis et al., 2008).

Next to the DEM extraction purposes, Airborne Laser Scanning (ALS) techniques can be used for monitoring vegetation change through time, forest classification and flood simulation (Antonarakis et al., 2008). The 3D-pointclouds that are measured from airborne LiDAR scans can be used to classify objects in high resolution and in a cost-effective way. In the Netherlands, the AHN (Actueel Hoogtebestand Nederland, or Up-to-date Height Model of the Netherlands) is acquired using airborne LiDAR. The AHN is a joint initiative from Rijkswaterstaat (Dutch national infrastructure authority), the regional water boards and provinces. The AHN offers a complete Digital Surface Model of the Netherlands which can be used for tree crown identification.

An airborne LiDAR system uses three data collection tools: the laser scanner, a GNSS (Global Navigation Satellite System) receiver, which measures the position of the aircraft and finally an Inertial

Navigation System, which is used to measure the roll, pitch and yaw of the aircraft (Leigh et al., 2009). Full-waveform LiDAR technology can record 1D signals representing multiple echoes caused by reflections at different targets (Guo et al., 2011). Figure 1 shows how the different objects on the surface can be identified by analysing their characteristic reflection intensity signals. Heights can be determined by measuring the waveform receival time on objects after the emitted pulse relative to the ground waveform receival time.

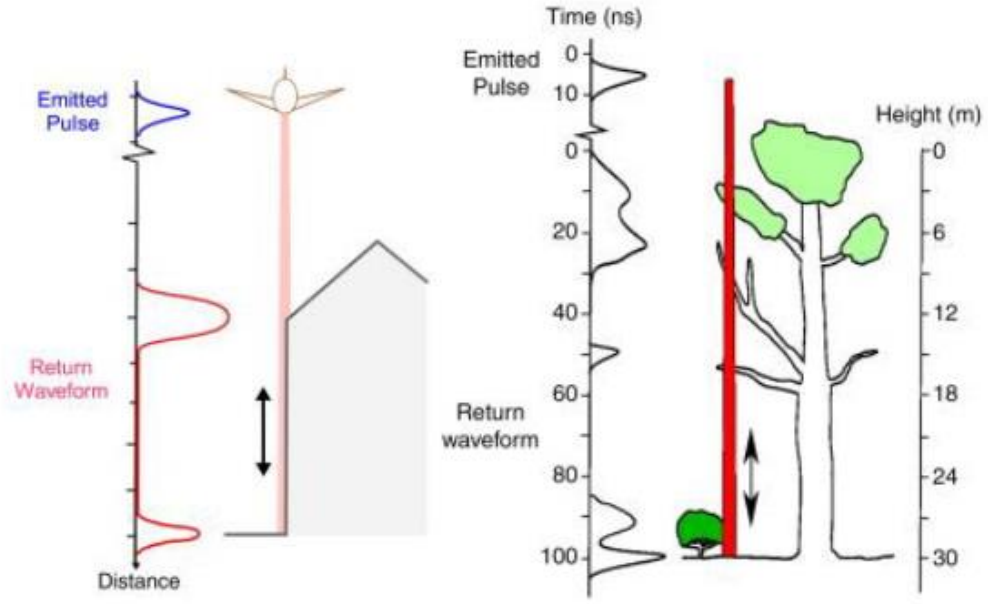

Figure 1: Airborne LiDAR classification methods (Guo et al., 2011)

The 3D-pointclouds are used to calculate both the Digital Surface Model, which describes the actual heights including objects such as buildings, and trees and the Digital Terrain Model, which only includes the ground surface without objects (Meijer et al., 2015, p. 17). In 2003 the first generation of the AHN (AHN1) was presented with a density of one height measurement per 1 to 16 square metres (Swart, 2010). In 2012 the second version (AHN2) was completed which has an average point density of 6 to 10 points per square metre and has an interpolated grid size of 0.5m (Van der Zon, 2013). The data acquisition for the newest generation (AHN3) is currently taking place and is expected to be finished by 2019. The tree crown delineation method developed by Alterra uses AHN2 and in urban areas between 30% and 50% of the trees that are existing are not identified by the model (Meijer et al., 2015, p. 53). With the introduction of the more detailed AHN3 it is likely that crown delineation can be more complete and more reliable.

1.1.2 Object-Based Image Analysis

"Object-Based Image Analysis (OBIA) is a sub-discipline of GIScience devoted to partitioning remote sensing (RS) imagery into meaningful image-objects, and assessing their characteristics through spatial, spectral and temporal scale" (Hay & Castilla, 2006). OBIA stands out compared to pixel-based approaches, because pixel topology is limited and current remote sensing image analysis largely neglects the spatial photo interpretive elements such as texture, context and shape, which results in lower classification accuracies (Hay & Castilla, 2006). When using OBIA in practice it is important to keep in mind that different resolutions of an image give different results. In low-resolution models, the resolution cells are larger than the elements, so there can by many objects per pixel, which makes the pixels easy to interpret because the differences are small (Haara & Haarala, 2002, p.557). In high-resolution models, one object will consist of multiple pixels, which offers more possibilities to observe variation. However, these resolutions require more powerful analysis methods and can result in over-segmentation, because more different textures are identified (Haara & Haarala, 2002, p. 557).

When applying OBIA to individual tree crown delineation Jing et al. (2012) state that there are two possible methods to deal with the different resolutions in order to prevent over-segmentation and under-segmentation. The first is a multi-scape approach, proposed by Thomas Brandtberg & Fredrik Walter in which first the tree crown contours were identified for each image scale after which a mean circle of curvature could be sketched (Brandtberg & Walter, 1998). The second option is an image pre-processing approach proposed by Le Wang (2008). In this approach, each band of a multispectral image is decomposed to obtain its approximation, horizontal, vertical and diagonal wavelet coefficients at multiple scales, after which a crown edge probability is derived for the horizontal and vertical coefficients and a multispectral image can be reconstructed (Wang, 2008). These methods however still have issues which are due to the various sizes of objects, the image filtering methods and the information integration at different scales (Jing et al., 2012).

1.2 Problem definition

Conventional tree inventory techniques are labour and cost intensive, while most algorithms for digital crown delineation methods are developed for specific site conditions (Ke & Quackenbush, 2017). There is a need for a standardized method that can deal with different environments and improves the monitoring efficiency for tree managers and urban planners (Verhaar, 2016). Tree-crown detection methods of deciduous trees are not fully studied and there is currently no standard framework for accuracy assessment of crown delineation (Ke & Quackenbush, 2017). The methods that are developed in the Netherlands by Alterra and NEO aim to cover all environments and tree species, however they are not without limitations.

The OBIA method by NEO has problems in dealing with the various sizes of trees, the image filtering and the different scales of images (Boombasis, n.d.). The DSM-method has problems with correctly identifying tree crowns due to the limited point density of AHN2 and therefore the coarse resolution of the resulting raster grid (Meijer et al., 2015). The Boomregister (2016) states that their

product has a 95% completeness in which less than 5% of the objects is incorrectly identified as tree crown, however trees under 9 meters in height with a crown diameter less than 4 meter have less completeness. Furthermore, trees smaller than 6 meters are not identified and for trees in rows the completeness is down to 80% (Boomregister, 2016). The method by Alterra has a completeness of 62.8% (Meijer et al., 2015, p. 44).

1.3 Research objectives

The general objective of this thesis is to create an improved tree crown identification method. To improve the shortcomings of the existing tree identification methods this thesis will analyse the characteristics of both the NEO based OBIA-method and Alterra based DSM-method. To identify what the strengths and weaknesses of these methods they will be compared at different compositions of trees and with different spatial resolutions. The strengths of both methods are then used in a new algorithm that aims to improve the results by combining the best practices. The best practices in this study are parameter and input based, meaning that the new hybrid method will be using the input datasets and tool parameter settings that are most suitable for identifying tree crowns. To determine what settings are most suitable, the results of the different methods are compared to a validation dataset. The best practices will be based on what input datasets and parameter settings result in the highest similarity to this validation set. In the end, the results of all methods will be validated by comparing them with the reference data to identify the most suitable tree crown identification method.

1.4 Research questions

To realize the objective, three main research questions must be answered:

1. How can the DSM- and OBIA-methods be compared for identifying individual trees?
2. How should the hybrid method be constructed?
3. What improvement is realized by the hybrid method?

Each of these research questions consists of several sub-questions that are used to answer the main research question.

How can the DSM- and OBIA-methods be compared for identifying individual trees?

- What characteristics of the DSM-method specify individual tree crown delineation?
- What characteristics of the OBIA-method specify individual tree crown delineation?
- How are these characteristics influenced by input-data and model parameter settings?

How should the hybrid method be constructed?

- What are the best practices of the DSM- and OBIA-method that should be used for an improved hybrid method?
- How can the best practices be combined into a hybrid method?

What improvement is realized by the hybrid method?

- Are the results of the hybrid method an improvement regarding crown area estimation?
- Are the results of the hybrid method an improvement regarding individual tree crown count?
- For what tree composition types are the results of the hybrid method an improvement?

2. Methodology

To obtain the best practices of the DSM- and OBIA-method relative to the validation dataset, the first step was to create the models based on Clement (Meijer et al., 2015) and Davids (2013). The second step was to compare the results for different input datasets and model parameters. Finally, the models were combined to create a new method that includes the best practices of both methods. In this chapter, the complete methodology will be explained, starting with an overview of the model framework, workflows and materials. The explanation of the steps and operations taken in the DSM-model will be presented in chapter 3. Chapter 4 consists of an explanation of the steps and operations of the OBIA model. The methodology will conclude with subchapter 2.5 on the validation process.

2.1 Framework

First the models of the DSM- and OBIA-method were created. The original OBIA-method uses the AHN3 pointcloud as input and the DSM-method uses AHN2 rasters with a horizontal resolution of 50cm. It is possible to extract the 50cm surface models from the pointcloud as well, but since the AHN2 data is from 2008, while AHN3 is from 2014, it shows a difference in the results. The next step was to change the pre-processing of the input datasets to create input datasets with the same resolution. The methods were compared for AHN2 at a resolution of 50cm and for AHN3 at a resolution of both 50cm and 25cm. The other datasets used in the analysis are: buildings from BAG (Dutch register for addresses and buildings), an aerial CIR (Colour Infrared) image and derivative NDVI (Normalized Difference Vegetation Index), were converted to these resolutions as well.

The workflow described in Figure 2 shows the inputs and parameters of the operations that were changed in the different stages of the analysis. Because the different methods use different was not possible to directly compare the differences in input for both models. To determine the best practices these inputs were for each model chosen individually based on their impact on the results. the DSM-method the parameter variables that were changed from the default are the neighbourhood size, the NDVI threshold and the roughness threshold. The neighbourhood size is the area on which algorithm searches for the highest pixels compared to their adjacent pixels. The method which determines the peaks of the trees will be explained in chapter

3.2 Peaks. As parameters both a small neighbourhood of 3 meters and a larger neighbourhood of 5 meters were chosen to compare the results to the default neighbourhood of 4 meters. The NDVI and roughness thresholds are the values for which the pixels are defined in the filters that will exclude those pixels from the image to reveal the remaining potential tree areas. More on these filters will be explained in chapter 3.1 Filters when discussing the DSM-method.

The most influential operation for the OBIA-method is the segmentation algorithm that defines the different segments of the inputs. The operational variables that are changed in the OBIA-method are therefore parameters of the Multiresolution Segmentation, which will be further explained in chapter 4.2 Segmentation when discussing the OBIA-method. The four parameters that are changed from the default are: the weights of the inputs of the multiresolution segmentation tool, the scale parameter that

defines the size of the segments, the shape of the segments and the compactness of the segments. These parameters define how many segments are covering a tree and what shape and size they take. The final phase of the conceptual workflow of Figure 2 shows that the aim is to make an improved method based on these models. Based on the best practices of the DSM- and OBIA-method a hybrid model has been created which uses the filters that are defined in the original DSM-method and uses these to define the input for the OBIA-method on the 25cm resolution AHN3 pointcloud. The filters of the DSM-method are compared to the classification-filters that are originally included in the AHN3 pointcloud dataset.

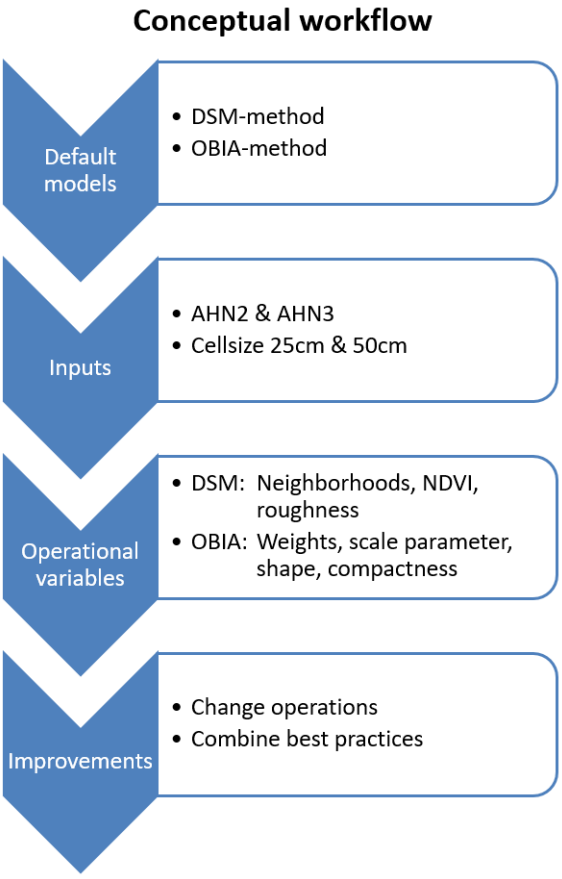

Figure 2: Conceptual workflow

Next to the conceptual workflow, Figure 3 shows the Operational workflow, which gives an overview of how different operational steps were taken in the DSM- and OBIA-method. The operational workflow indicates the order of the different processing phases for each method and how they result in the best practices, that were used as feedback for the input parameters. The best practices are determined by comparing the results to the validation dataset for all different inputs and model parameters. Each phase that is visualised in Figure 3 contains different operations, of which the details will be further explained in the chapters 3 and 4 on the individual methods. The model also shows that

the OBIA-method uses a different approach for the crown delineation. In this method, the individual trees are classified as single trees, part of a row or part of a group, which will be defined in chapter 4.4 Finally, they are merged together to create the final dataset. The DSM-method doesn't make this distinction, so the results don't indicate the type of the individual tree.

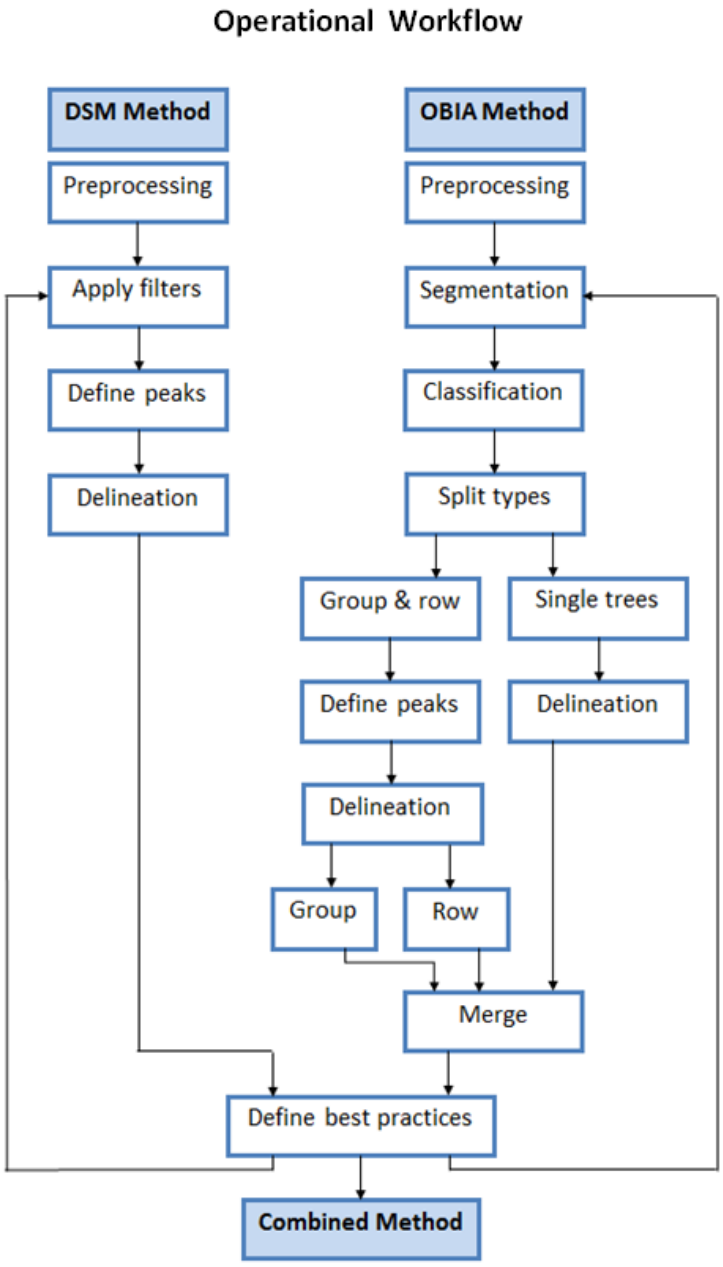

Figure 3: Operational workflow

Most of the phases in Figure 3 are processed in ArcMap, developed by ESRI, however some of the Pre-processing steps of the OBIA-method are done with LAStools, developed by rapidlasso GmbH, which was used to create a pointcloud with heights relative to the ground level. LAStools is a software package that can be used to unzip and process pointcloud datasets. The AHN data is available as

datatype .laz, a compressed pointcloud that can be converted in LAStools to .las, which can be used as input in eCognition, developed by Trimble. The eCognition Developer software was used for the Segmentation and Classification steps of the OBIA-method. Statistics on the generated individual trees for the different methods were calculated in MS Excel.

2.2 Tree definitions

As indicated in the previous chapter, the OBIA-method divides the individual trees in three composition types: single trees, trees part of a row or lane and trees as part of groups. For the model to work these composition types need to be defined. The OBIA-method is based on the thesis of Lucien Davids (2013), however the aim of Davids was not to identify individual tree crowns, but to define small green landscape elements. Therefore, the trees in a row or group are not treated as individuals but as a part of a greater entity. The assumptions from Davids (2013, p. 31) that are used in this thesis as well are that the crowns of single trees don't touch the boundaries of the crowns of other trees. When there are more than two single trees that share boundaries, the trees are classified as part of a group. For a row Davids (2013, p. 31) assumes that the length of the object is greater than the width and that a lane consists of multiple rows. The individual trees within a group or row are not defined by Davids, so these assumptions alone are not clear enough to define when a tree is part of a row or part of a group.

The Boomregister uses a similar definition as Davids, with the addition that a row of trees must be in close proximity to a road (BoomBasis, n.d.). The Boombasis is used in this thesis as comparison for the final results and as inspiration for the method to distinguish individual trees from a row or group. The study area, which will be described in chapter 2.1.3, is largely covered by a park and does have lanes of trees that are not in close proximity to a road, but still form a row. Therefore, in this study the following rules to indicate whether tree that is part of a row have been used:

- The difference in length and width of the object is at least 10 meters.
- The individual tree in a row shares a boundary with neighbours in maximum eight directions as indicated in the Moore neighbourhood in Figure 4 (White & Kiester, 2008).
- The individual tree in a row shares a maximum of one boundary in each direction.

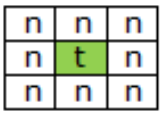

Figure 4: Example of maximum directions and neighbours for a tree to be classified as a row

As defined by these rules there is no distinction between a tree in a lane, which is defined by multiple rows, and a tree that is within an individual row. Both trees will be classified as part of a row. When the definitions of a single tree and a row are clear, the trees that don't fall into these categories are classified as part of a group. An example of each tree composition type is visualized in Figure 5.

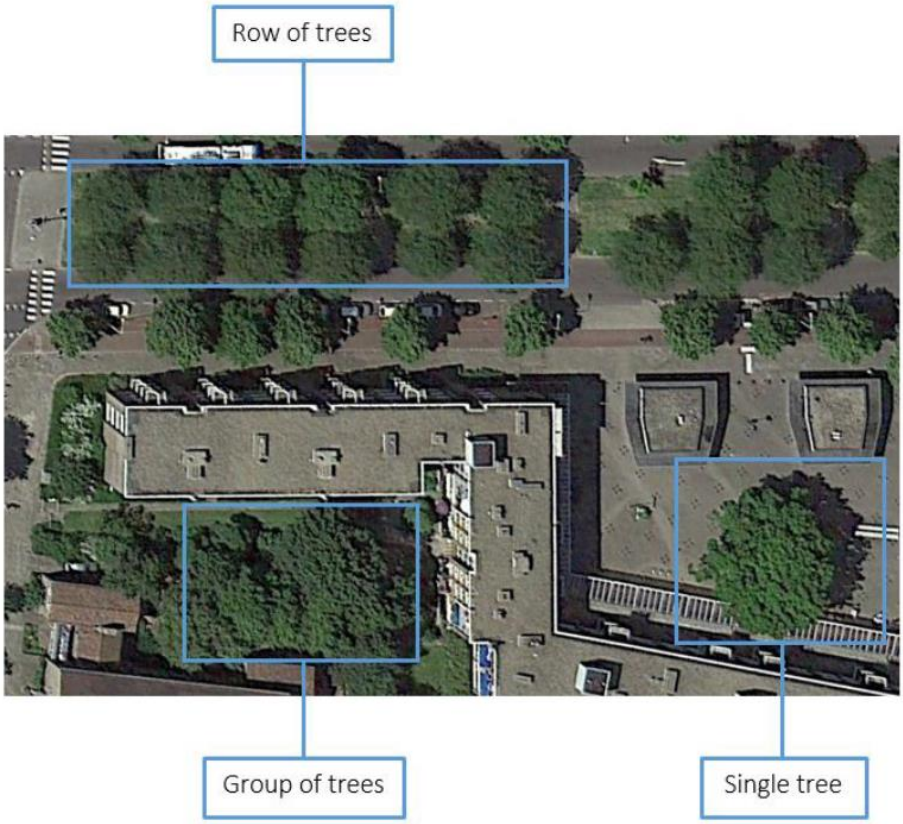

Figure 5: Tree compositions (Google Earth 2013, Den Haag)

2.3 Study area

The data from AHN3 is not available for the entire Netherlands, so the possible locations to apply the model were limited. Furthermore, the study area must have reliable reference data available to make a comparison between the results of the methods. Den Haag meets these criteria, because it has a reliable database which includes information on tree locations for several years as well as the aerial photographs that are necessary for the OBIA. More importantly, Den Haag is willing to share their data so it can be used as a reference when validating the different methods. In Figure 6 the study area within Den Haag is presented, where the area around the Zuiderpark is chosen as location to focus on. The study area is limited to the Zuiderpark area, because it would take too much processing time to apply the models on the entire municipality of Den Haag. The area around the Zuiderpark is chosen, because it offers many instances of all tree composition types in both the urban environment and the park itself. The different environments are interesting, because they cause different challenges, for example the proximity to buildings in urban areas, or the different green elements in the park.

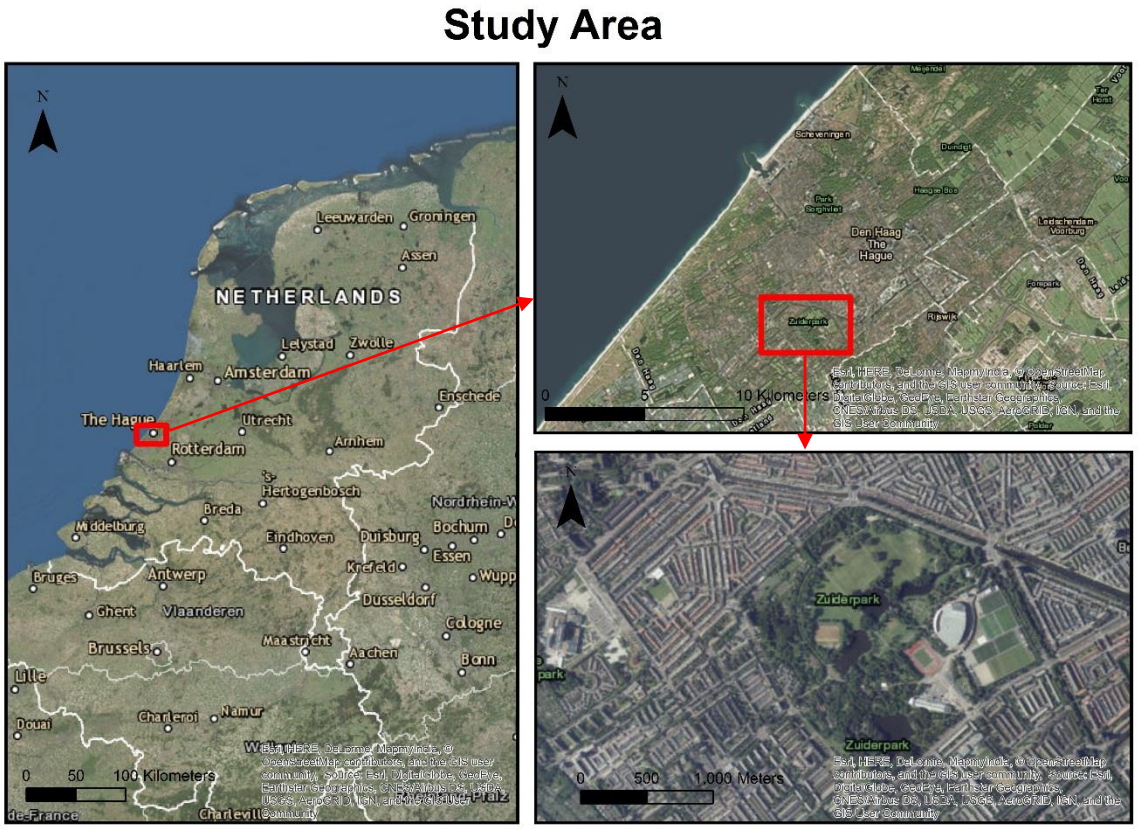

Figure 6: Study area Zuiderpark, Den Haag (ESRI World Imagery)

2.4 Input data

The most important data that is used as input for both methods are versions 2 and 3 of the height model of the Netherlands AHN2 and AHN3. The AHN2 is used as default input for the DSM-method for the AHN3 is used as input for the OBIA-method. For the comparison between the methods, the different AHN versions are used to determine their influence on the results. The AHN2 dataset for Den Haag was acquired in 2008 and has an average point density within the study area of 17 points per square meter (Van der Zon, 2013). The AHN3 dataset for Den Haag was acquired in 2014 and has a measured average point density within the study area of 41 points per square meter. In Figure 7 the difference in density is visualized for a single tree. The top row shows the view from the side for both AHN2 and AHN3, the bottom row shows the view from above for both datasets where the points are coloured according to their elevation. The images in Figure 7 show how influential the point density is for the identification of the shape of the tree, but also for the accuracy in the determination of height and volume. Therefore, trees can be more accurately identified in datasets with a higher point density.

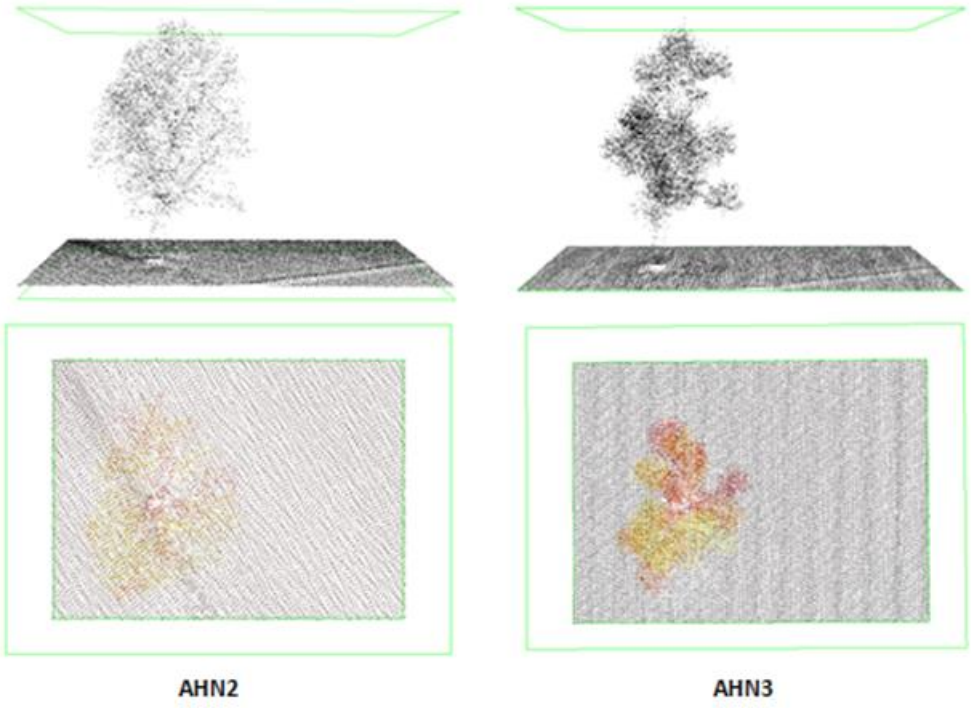

Figure 7: Comparison between AHN2 and AHN3 pointclouds

Another input dataset that is used is the buildings register of the Netherlands. This dataset is used for the buildings-filter of the DSM-method, which will be further explained in chapter 2.2. This BAG-dataset, managed by the Dutch national cadastre, has frequent quality checks and updates, which makes it very reliable. The BAG provides information on the status and location of buildings in the Netherlands and is available as vector-data. For the buildings-filter a selection was made to eliminate demolished buildings and buildings that were not under construction at the time of AHN acquisition. This selection was made for the versions of AHN2 in 2008 and for the versions that use AHN3 in 2014. In the DSM-method this building-filter is used to determine the areas that are not covered by trees. The buildings are removed from the height models to limit the objects that were incorrectly identified as trees.

A Colour Infrared (CIR) image was used as input dataset to calculate the NDVI and for the multiresolution segmentation of the OBIA-method as will be explained in chapter 2.3. The dataset is from 2016 and is provided by Beeldmateriaal and PDOK. It consists of a RGB and false colour orthographic aerial image with a horizontal resolution of 25cm covering the Netherlands (Nationaal Georegister, 2017). Orthographic images are constructed in an orthomosaic by combining a large number of aerial images, corrected on location and terrain (Mills & McLeod, 2013, p.101). Figure 8 shows that the production of these orthographic images is not flawless. In the figure, the left side shows the CIR image and the view direction of the same building on Google Street View on the right side of the image. It appears on the CIR image that the building is leaning on an angle over the street, while on Google Street View this doesn't seem the case. These deviations are more apparent at higher objects, so higher

trees might be more affected than small trees. The CIR orthographic image is used for calculating the NDVI, which is used in the DSM-method as a filter to exclude areas below a certain threshold. In the OBIA-method both the CIR-image as the derived NDVI are used as input for the multiresolution segmentation. The deviations will therefore have an influence in the results of both methods.

Figure 8: Example of deviation in the CIR-image (Left: Nationaal Georegister 2016, Right: Google Street View 2014)

2.5 Validation method

To determine what method and optimal parameter settings deliver the best results, the identified tree crowns are compared to a validation dataset. The results of the different tree crown identification methods are determined in two ways. The first way is by comparing the identified number of trees to the tree locations as determined in a validation dataset. Any difference is summed up in the count deviation for the different tree types as shown in Appendix III. The deviations are determined by visually comparing the number of polygons that intersect the validation tree. The results are then calculated as similarity percentages to the validation set. Using percentages instead of absolute numbers made it possible to calculate average similarity scores, which take both the count deviation and area deviation into account. For some purposes, the count is more useful, for example for making an inventory of the number of trees in an area. For other purposes, the crown area is more useful, for example when estimating biomass or shade. The average similarity percentage is used to see what method performs

best overall. In Figure 9 an example is shown of a count deviation for a single tree. The example shows a count deviation of 1 with the validation dataset.

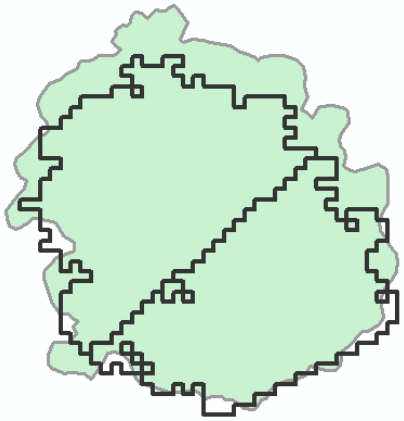

Figure 9: Example of a count deviation of 1 for a single tree

The second way to determine the performance of the crown identification method is by comparing the crown area to the validation method. In the example of Figure 9, the areas of both identified crowns have to be combined, because the individual crown areas are not relevant when determining variables like for example vegetation mass or tree shadows. When calculating the combined crown areas of a group of trees, as shown in Figure 10, it becomes clear that validating the individual crowns is impossible. In this example, the same method as in Figure 9 is used, but fewer trees have been identified relative to the validation set, resulting in a count deviation of 4. It is impossible to determine what part of an identified tree crown belongs to a tree in the validation set; therefore, for all groups, the areas are combined to compare the total crown area of the datasets. For the rows of trees, both the individual tree crown areas as the total grouped crown areas are calculated.

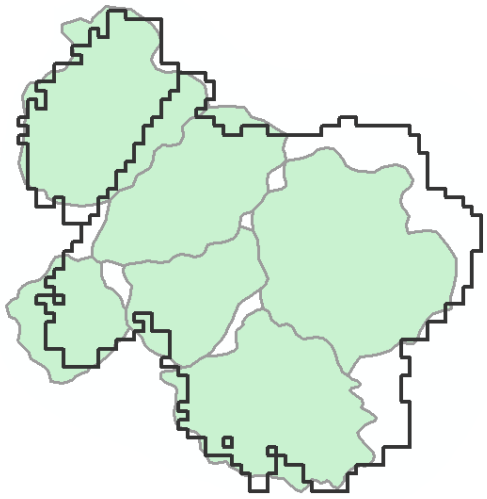

Figure 10: Example of a count deviation of 4 for a group of trees

2.5.1 Validation criteria

The reliability of the validation data depends on the time of acquirement and on the tree delineation method. The comparison between the method results and the validation data would be best if the date of acquirement of the validation data is the same as the date of the acquirement of the model input dates. Furthermore, the delineation method in the validation dataset would ideally be 100% correct. That way the tree crown deviations between the validation dataset and the different method results can be fully attributed to the performance of the methods. To obtain a validation dataset, a high-resolution aerial image from the same time period as the input data had to be obtained to manually delineate the tree crowns. The resolution needed to be high enough to visually differentiate the different tree crowns.

The AHN datasets used as input for all methods are acquired between winter and summer and it is not clear what the precise dates are for each location. This makes the validation less reliable, because it is not clear in what stage of the leaf growth cycle the AHN data was acquired. For the manual delineation method, there are different upsides of using an image taken in summer or one taken in winter. In summer, it is easier to visually differentiate the different species based on leaf colours. However, in winter images the different branches are visible, which makes it easier to differentiate between trees of the same species.

2.5.2 Den Haag

As validation location and therefore study area, the municipality of Den Haag was chosen, because it fulfilled all criteria. The Zuiderpark area, as shown in Figure 6, was chosen as location for the study area, because it provided a challenging mix of urban space and green space, where different landscape elements could influence the model. Most importantly however, the area contains a large variety of single trees, rows and groups. It was necessary to have all tree composition types frequently in the same area, because otherwise a larger study area, or more study areas, needed to be chosen, which would have caused an inconvenient increase in processing time. The delineation of the trees is done manually in ArcGIS by visually identifying the tree boundaries on the high resolution (5cm) aerial image as seen in Figure 11 for a row of trees.

Figure 11: Example of validation delineation for a row of trees

Next to the high-resolution aerial images, the municipality of Den Haag also provided the locations of the stems of the trees, which were used to help with the delineation and to exclude trees where no stem was present. The aerial images did show some deviation from the AHN and CIR Ortho locations. Figure 12 shows an example in which the crown from the CIR ortho image is extending 2 meters further to the south than the crown in the validation image. Therefore, the validation data is used to compare the tree areas of the results of each method is not suited to compare the locations.

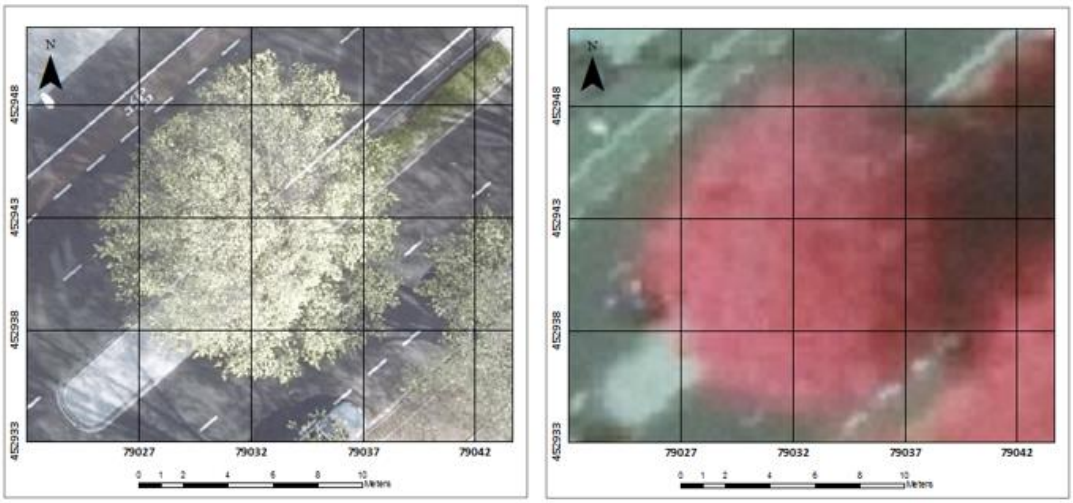

Figure 12: Difference between validation image and CIR image

The AHN3 is from 2014, but the aerial images were only available for 2013 and 2015, so both years are taken into account. In some cases, like in Figure 13, the tree from 2013 is no longer standing in 2015. Those trees are not taken into account in the validation, because it is not clear if it was cut down before or after the AHN3 data was obtained. Both images from 2013 and 2015 are from spring, which is the same time of year as the AHN2 and AHN3 datasets are obtained in Den Haag (Actueel Hoogtebestand Nederland, n.d.).

Figure 13: Example of differences in 2013 and 2015 validation image

3. DSM-method

In this chapter the characteristics of the DSM-method are analysed in order to determine how individual tree crowns are identified using Digital Surface Models as input. The tree crown extraction algorithm that is used as the default DSM-method is created by Alterra and uses the AHN2 DSM and DTM as input dataset (Meijer et al., 2015). In this thesis, the method is using both AHN2 and AHN3 according to the latest version of the description of the extraction algorithm, which uses the BGT and NDVI as filters (Meijer et al., 2015, p. 16 – 20). The first step in the algorithm is to create these filters that define the area that covers the potential trees. The second step is to determine the peaks of the remaining potential tree area. Finally, these peaks are used to delineate the crowns around them.

3.1 Filters

In the method, there are four filters that define the potential tree area by excluding the areas that fall below a certain threshold that defines the presence of trees. The four filters are based on: the presence of buildings, roughness, NDVI and height. As explained in chapter 2.4 the BAG is a dataset that provides vector data for buildings in the entire Netherlands. For both AHN2 and AHN3, a selection was made to exclude buildings that were demolished or not yet finished. After testing the model, it became clear that a lot of the edges of buildings were still apparent and classified incorrectly as trees. Therefore, to compensate for the flaws in the AHN datasets and in the orthographic image, a buffer of 1 meter was created around the buildings to eliminate this issue. Finally, the buildings were dissolved and converted to a raster to create the first filter.

The roughness filter was created to remove relatively smooth areas, so trees and other vegetation that have more variation in height on smaller areas remain. The filter is created by calculating the standard deviation of the DSM height values in an area of 3x3 cells and removing the areas that are below the threshold (Meijer et al., 2013, p. 17). The NDVI was calculated using the near-infrared and red bands from the orthographic CIR image following the equation:

$$NDVI = \frac{(NIR - R)}{(NIR + R)}$$

This results in values varying between -1 and 1 where values close to 1 indicate the presence of vegetation and values close to -1 indicate that no vegetation is present. The threshold for the NDVI filter is set to pixel values ≤ 0.2 to filter the pixels that are unlikely to be vegetation (Meijer et al., 2013, p. 19). The height filter was created by calculating the Digital Elevation Model from the DSM and the DTM. This DEM contains the heights relative to the ground level, so the filter was created by removing heights > 4m to filter out objects which have a height below the threshold to be considered trees (Meijer et al., 2013, p. 19). Finally, all filters were merged to a new raster to create a combined filter that removes most areas where trees aren't located. The left side of Figure 14 shows the result of the combined filter for a part of the study area for AHN3 at 50cm resolution. On this map, it is already possible to visually identify different types of tree compositions, however small objects such as lampposts are still present as shown on the right side of Figure 14.

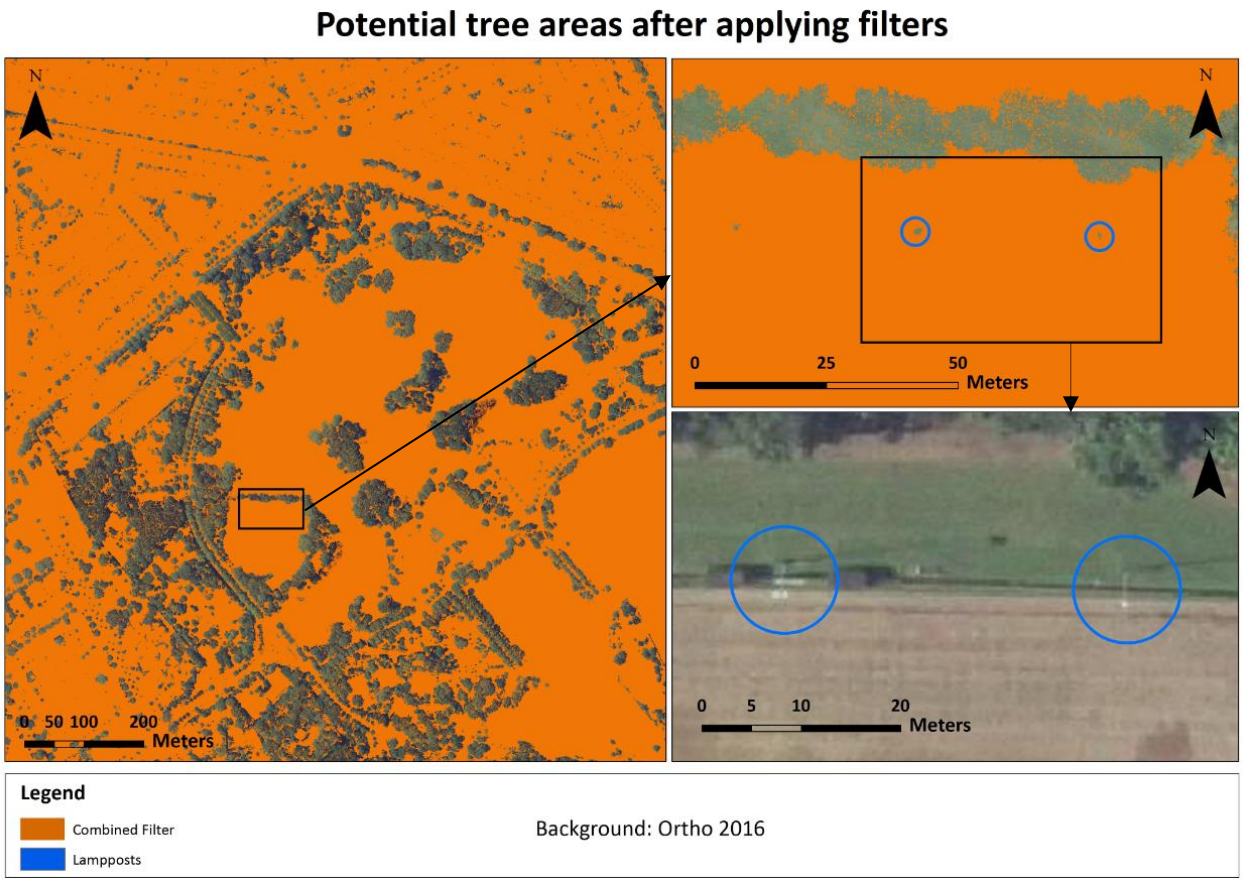

Figure 14: Potential trees after applying filters

3.2 Peaks

The combined filter is converted to a mask, used to extract the values from the DEM. This results in a height model which only covers the potential tree area. Clement (Meijer et al., 2015, p. 19) used the following description of how to determine the peaks: *"the raster cells with peak values are determined by looking at what cell values differ the most (upward) from the average normalized height"*. Based on this a focal statistics method was used to determine the maximum value within a certain neighbourhood setting. Two different radius neighbourhoods were used, one with a 4-meter radius for small trees and one with a 6-meter radius for high trees. The focal statistics tool iterates over all cells in the raster dataset and creates a new raster on which the maximum values of the specified neighbourhood are assigned to a cell. The DEM height values were subtracted from these maximum values which results in all peaks having the value 0. The original DEM height values were assigned to these cells and converted to point data to identify the peaks according to their relative height. Finally, a selection was made to identify peaks > 15m from the dataset which used a 6-meter radius as neighbourhood and <= 15m from the dataset which used a 4-meter radius as neighbourhood. These different settings were used, under the assumption that higher trees cover a larger area, so they should have a larger neighbourhood as well. The different selections were merged to create the final peak dataset in point vectors.

3.3 Delineation

To identify the individual tree crowns in a row or group with multiple trees it is necessary to determine what part of the potential tree area can be attributed to a single peak. In the report on the DSM-method from Alterra, the following method is chosen: *"The individual crowns in an area with multiple peaks are determined by constructing zones around each peak: the fragmentation. The zone around a peak consists of the set of cells that are located closer to the peak in that zone than to another peak. The zone around a peak thus contains the cells with the smallest Euclidean distance to the cell with the peak value"* (Meijer et al., 2015, p. 17). The tool that was used in ArcMap to determine the individual zones around the peaks is the Euclidean Allocation tool, which returns a raster of cells that have are grouped by their distance to the peaks. The next step was to convert the raster to polygons and to determine their size by adding geometry attributes. Clement (Meijer et al., 2015, p. 18) then made corrections on the sizes of these zones where smaller clusters are combined to larger zones. The Eliminate tool was used in ArcMap to dissolve areas smaller than 30 square meters to the neighbour to which they share their largest border as seen in the example from the AHN3 50cm resolution version in Figure 15, in which the different colours represent different objects. Finally, the new geometry attributes are calculated to obtain the area of the tree crowns.

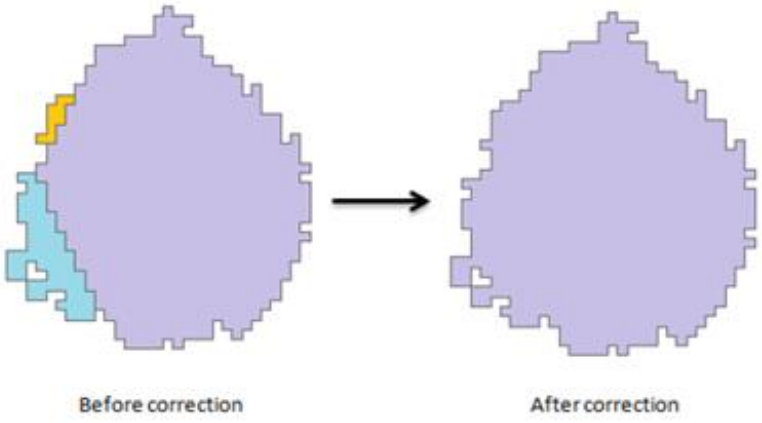

Figure 15: Example of Eliminate tool in ArcGIS for a single tree

4. OBIA-method

In this chapter the characteristics of the OBIA-method are analysed in order to determine how individual tree crowns are identified using aerial images as input. The method using the object based image analysis is more complicated to recreate than the DSM-method, because it was necessary to use different software to process the data and there was no report available like the report from Alterra used in the DSM-method. The master thesis of Lucien Davids (2013) describes the segmentation and classification phase of the OBIA method. The determination of the peaks is based on the DSM-method and the delineation phase is done by using a 'growth' algorithm that will be further explained in chapter 4.5 on the delineation. First, the pre-processing phase of the OBIA processing steps will be explained, followed by the segmentation, the classification, the peak determination and finally the delineation.

4.1 Pre-processing

Before the object based image analysis could start, it was needed to merge the AHN2 DSM and DTM in LAStools using LASmerge in order to obtain the complete pointcloud of the area. AHN3 is already delivered as the complete dataset so it was not necessary to repeat this process for AHN3. After the merging, both datasets were clipped on the study area to reduce the processing time. It is possible to classify the pointclouds in LAStools before using the segmentation tool as shown in the method from Davids (2013, p. 38). First, the LASground tool is used to classify the ground points by calculating the elevation of the last returns of the LiDAR dataset (rapidlasso GmbH, n.d.). These can be used as input for the LASheight tool, which is used to calculate the relative heights from the points to the ground. The result can be used to convert the pointcloud to a DEM raster. Finally, the LASclassify tool is used to determine the four classes: Ground, Buildings, Vegetation and Other/Unclassified (Davids 2013, p. 39). LASclassify aims to find neighbouring points that are at least 2 meters above the ground and form roof or tree regions (rapidlasso GmbH, n.d.). Figure 16 shows the results of this classification. The green area represent vegetation, orange areas represent buildings, brown areas represent bare earth and grey areas are unclassified. This method does not seem very accurate, because the misclassification of vegetation as buildings is clearly visible. Therefore, in this study a different classification method will be used after the segmentation that will be described in chapter 4.3.

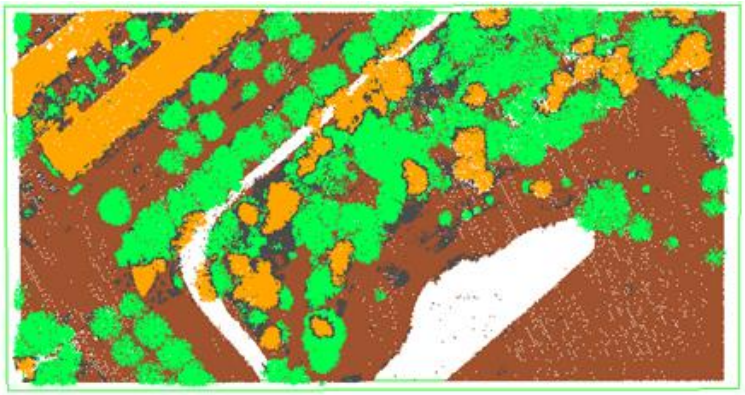

Figure 16: Misclassification in LAStools

After the results are pre-processed in LAStools the .las pointcloud files are used as input in eCognition Developer. Within eCognition the pointcloud is converted to two raster datasets. The first is a DEM, derived from the maximum of all returns of the pointcloud. This means that if there are multiple points within a specified raster cell, in 25cm or 50cm resolution, the elevation of the highest point is taken as attribute. The second raster converted from the pointcloud is the maximum number of returns from all returns of the pointcloud. Figure 17 shows that tree crowns have a relatively high number of returns, so the maximum number of returns for each raster cell is likely part of a tree crown. This is true for the AHN data as shown in Figure 18 in which the number of returns are visualized in a greyscale, where black represents a low number of returns and white represents a high number of returns.

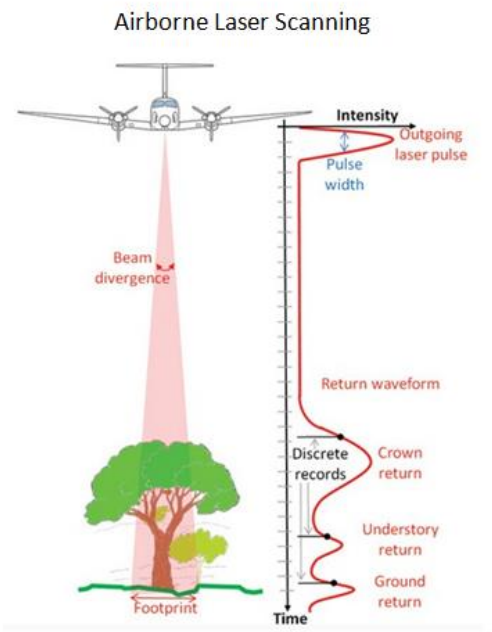

Figure 17: Airborne Laser Scanning (Fernandez-Diaz, 2011)

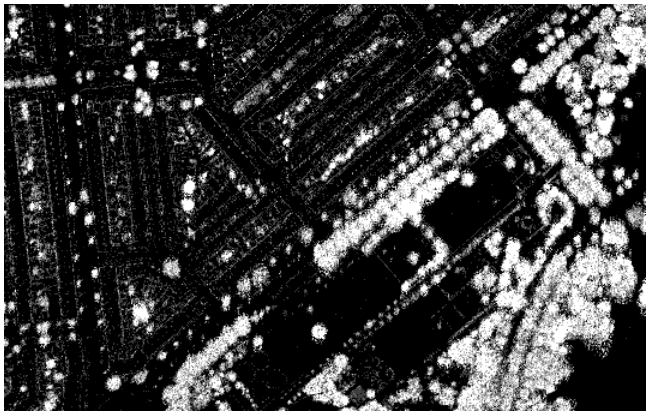

Figure 18: Number of returns from LiDAR image

The created rasters now need to be interpolated to remove missing data from the dataset for the segmentation to work best (Definiens, 2009). For the interpolation, first a new, temporary raster is created which will contain objects, classified with the values for elevation in meter or number of returns. Then, a loop is created to identify unclassified objects and assigning them the mean values of their neighbours. This loop is carried out until all objects are classified. When there are no unclassified objects left, the temporary raster layer is saved to a new layer and deleted from the workspace. These new interpolated elevation and number of returns rasters are now ready to be used as input in the segmentation algorithm.

4.2 Segmentation

The segmentation of an image refers to the process of partitioning a digital image into multiple segments, where sets of pixels are combined based on certain criteria of homogeneity (Davids, 2013, p. 35). The segmentation process is the defining part of the Object Based Image Analysis, because these multiple segments are the image objects generated from the homogeneity criteria (Darwish et al., 2003). There are different segmentation techniques that can be used within the eCognition software package. Figure 19 shows examples of different top-down segmentation techniques: chessboard segmentation (a), quadtree based segmentation (b), contrast filter segmentation (c) and contrast-split segmentation (d) (Davids, 2013, p. 37).

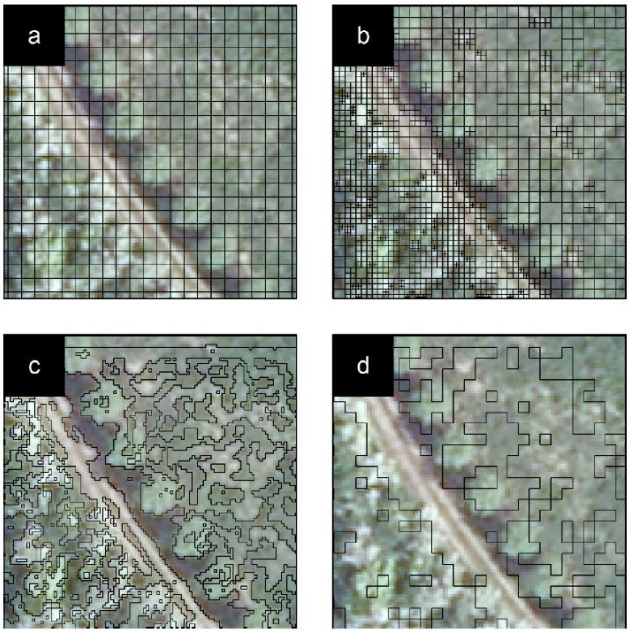

Figure 19: Top-down segmentation methods

Chessboard segmentation is the simplest segmentation technique that creates the objects according to a defined square size and doesn't take any information from the image into account. The quadtree based segmentation technique uses square objects as well, but the size of the squares is defined by the variation of pixel values in the image. The contrast filter segmentation uses a combination of two pixel filters to create a thematic raster layer based on the shape criteria and the lower and upper threshold of the filters (Landmap, n.d.). Finally, the contrast split segmentation technique can be used to detect edges between pixels with high and low values and is based on a threshold that maximizes the contrast between these values (Davids, 2013, p. 41).

Next to the top-down segmentation techniques shown in Figure 19, there are bottom-up techniques that perform segmentation of the complete image and group pixels to spatial clusters that meet certain criteria of homogeneity or heterogeneity (Yan, 2003, p. 16). In Figure 20: Bottom-up segmentation methodsFigure 20 examples of different bottom-up segmentation techniques are shown: multiresolution segmentation (a), multi-threshold segmentation (b) and spectral difference segmentation (c) (Davids, 2013, p. 37). The difference between the top down and bottom up techniques is that top down methods are knowledge driven, where the algorithm tries to find the best processing approach to extract the desired objects (Yan, 2003, p. 16). The bottom up methods are data driven and object oriented, where the algorithm performs a segmentation of the complete image and the user determines what the generated objects represent (Yan, 2003, p. 16). The multiresolution segmentation is a region-growing technique that merges pixels together based on their heterogeneity in a pairwise clustering process (Yan, 2003, p. 17). The multi-threshold algorithm splits the image object domain and classifies resulting image objects based on a defined pixel value threshold (Middleton et al., 2015, p. 145). The spectral difference method is designed to refine raw segmentation results and merges two neighbouring objects if the difference between their average intensity is smaller than a pre-defined parameter (Dezsö et al., 2012, p. 111).

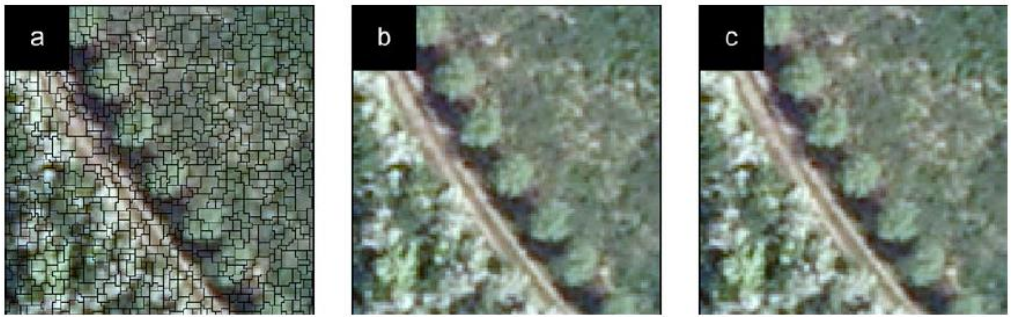

Figure 20: Bottom-up segmentation methods

In this study, a multiresolution segmentation technique was used to identify the tree objects, because it makes it possible to compare the heterogeneity of pixels using different input datasets, resulting in a great variety of information that can be derived from each resulting segmented object (Yah, 2003, p. 54) The basic principle of multiresolution segmentation is to make use of important

information (shape, texture and contextual information) that is present only in meaningful image objects and their mutual relationships (Darwish et al., 2003). Figure 21 shows the concept flow diagram of how multiresolution segmentation works and how the parameters will influence the results. Multiresolution segmentation is very suitable for identifying trees, because it is possible to combine different raster layers that each have characteristic features that indicate the presence of trees. The datasets that were used as input for the analysis are the red, green, blue and nir bands of the CIR image, the derived NDVI, the interpolated elevation raster and the interpolated number of returns. The elevation and number of returns were given the biggest weights, followed by the NDVI. The different bands of the CIR image are given lower weights for identifying tree crowns, because the most important bands for identifying vegetation are already included through the NDVI.

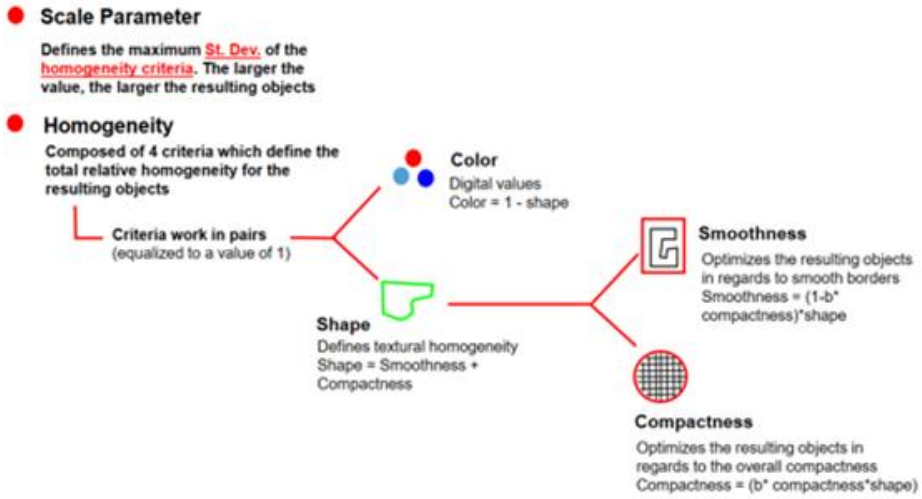

Figure 21: Multiresolution segmentation concept flow diagram with operational parameters (Wageningen University, 2014)

Figure 22 shows an example of the multiresolution segmentation technique for a single tree with as background the grey-scaled pixel values of the CIR red band. The different image objects are more suitable for tree identification, which was done by classifying the individual objects.

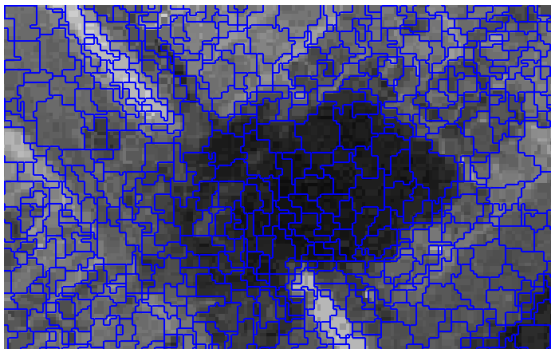

Figure 22: Example of multiresolution segmentation for a single tree

4.3 Classification

For the classification within eCognition, the different segments were identified as trees for the rasters of NDVI, elevation and number of return thresholds. The average pixel values of the segments are extracted from these rasters and the thresholds were set similarly as the filters from the DSM-method. The elevation threshold was set at > 4 meter, the NDVI must be > 0.2 and the mean number of returns, which was not used in the DSM-method, was > 2. An example of the classification results for a single tree is visible in Figure 23, where the results are shown at grey scaled pixel values of number of returns (a & b) and at grey scaled pixel values of NDVI (c & d). In the image a & c show the segmentation results, while in b & d the classification is presented.

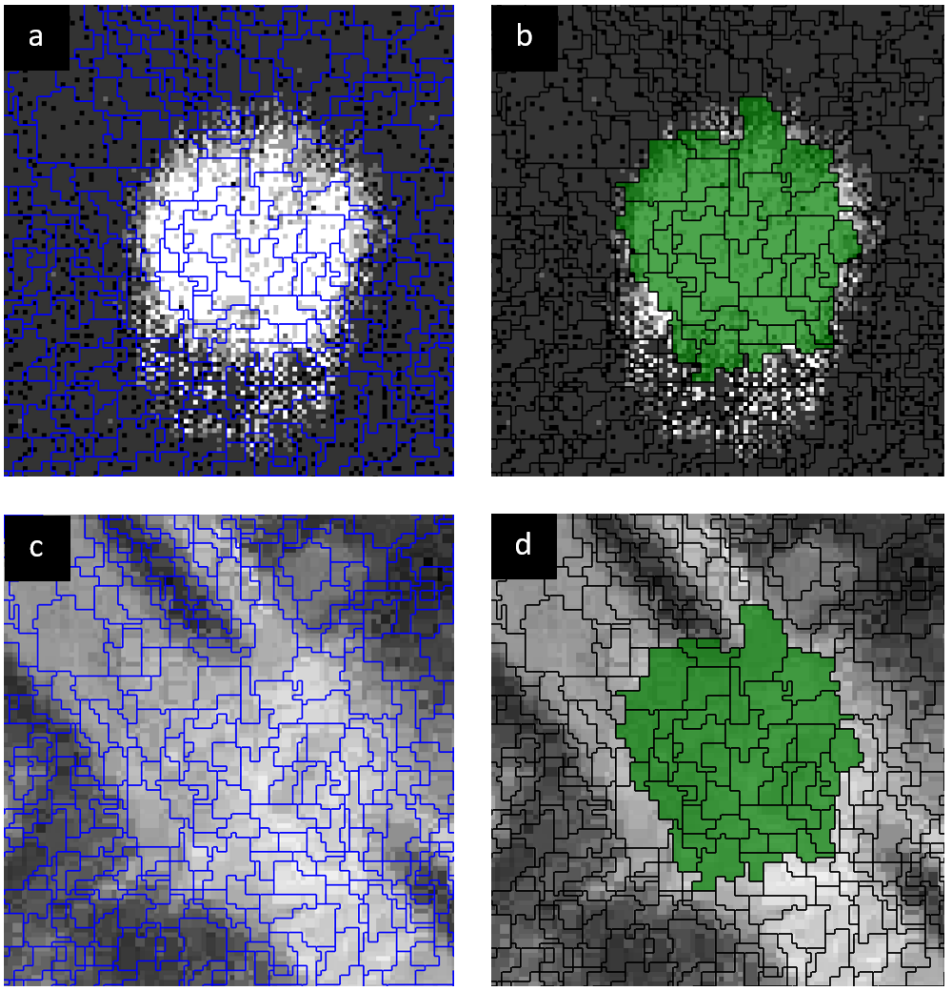

Figure 23: Example of classification results for a single tree

In the example in Figure 23 it is possible to visually identify a single tree. In Figure 24 the classification results are shown for multiple trees around a football field using a grey scaled NDVI as background. Here it is clear that when looking at rows or groups, it is not possible to identify an individual tree from a group, based on the different segments. Therefore, the results from the eCognition classification are not suitable for determining the results for rows and groups directly. Within ArcMap, all segments were merged and recombined to create meaningful objects from the individual segments (Davids, 2013, p. 38). This merge algorithm makes it possible to identify the single trees, based on the resulting size of the polygons and shape of the bounding geometry.

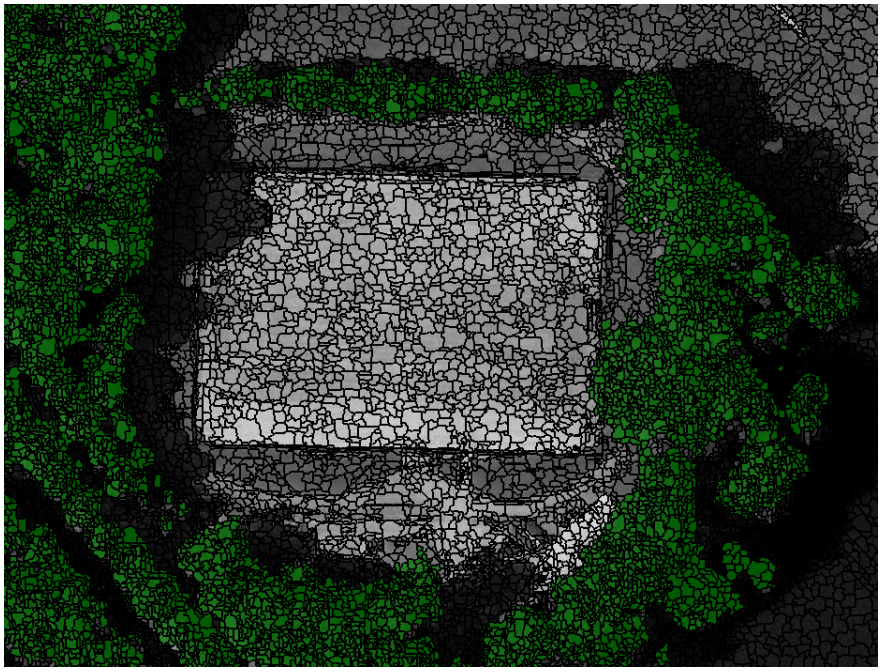

Figure 24: Example of classification results for larger groups of trees

4.4 Peaks

After the single trees were identified, their polygons were separated from the segmentation dataset. For the segments that cover rows and groups, the maximum elevation within a segment was calculated using the zonal statistics tool on the interpolated elevation raster. The peaks were then determined in a similar way to the DSM-method explained in chapter 3.2 using the focal statistic tool. There are however some differences in the two methods. For the OBIA-method the same neighbourhood radius of 4 meter was used for all peak heights and the resulting peaks were not point vectors but the polygon segments resulting from the image analysis. Another difference is that the OBIA-method used four categories of tree height instead of using two of trees > 15m and trees <= 15m. For the delineation, the OBIA-method used a similar technique as used in the Boombasis, where a growth algorithm is used to identify the single trees. Critical to this technique is the assumption that larger trees should have priority in growth (Wigger Tims, personal communication, March 7, 2017), so the peaks were divided in categories over 25

meter, between 15 and 25 meter, between 10 and 15 meter and between 4 and 10 meter. When the peaks were identified, it was possible to execute the delineation algorithm.

4.5 Delineation

For the delineation of the individual tree crowns a growth algorithm is created based on the Eliminate and Merge tools in ArcMap. The algorithm starts at the peaks and grows until all remaining segments are dissolved into a neighbouring peak. In Figure 25 an example of the growth algorithm for a group of fourteen peaks is given. The peaks are merged with their neighbours to which they share the largest boundary using the elimination tool. This elimination loop runs until there are no changes in number of polygons between the new datasets. Using this method, it is possible to make a more reliable estimation of the shape and area of the tree crown compared to the Euclidean distance algorithm used in the DSM-method. The delineation is not just based on the pixel distance to the peaks but includes the segments that are based on the variables specified in the multiresolution segmentation. When the delineation loop was complete, the groups and rows were identified in the same way as the single trees. Then all different types were combined into one dataset and the final step was to add the geometry attributes to determine the peak area.

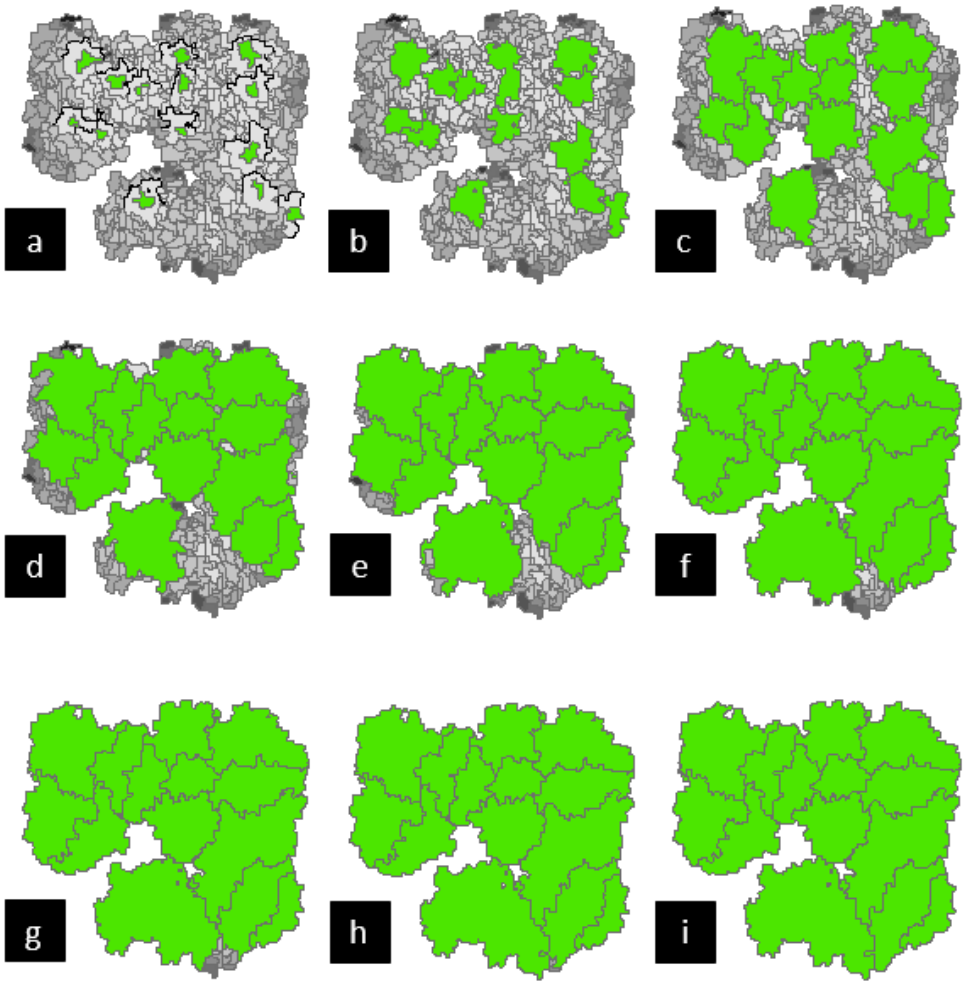

Figure 25: Example of the growth algorithm for a group of trees. (a) peaks over 25 meter, (b) new peaks over 20 meter, (c) new peaks over 15 meter, (d) 1st run all peaks, (e) 2nd run all peaks, (f) 3rd run all peaks, (g) 4th run all peaks, (h) 5th run all peaks, (i) 6th run all peaks

5. Results

In this chapter the results of the DSM-method and OBIA-method are presented. In the previous chapters, the default DSM- and OBIA-methods have been recreated according to the models as developed by Jan Clement (Meijer et al., 2015) and Lucien Davids (2013). In both these methods different input datasets and model parameters will have an influence on the results. To determine how the characteristics of both methods are influenced by input-data and model parameters, the results of each method have been compared to the validation dataset using different settings. For the DSM-method the chosen parameter settings will be explained in chapter 5.1, followed by a comparison to the validation dataset in chapter 5.2. The parameters of the OBIA-method are presented in chapter 5.3, after which the comparison to the validation dataset is presented in chapter 5.4. The results relative to the validation dataset are presented in different subchapters for single trees, rows of trees and groups of trees.

The second research objective is to determine how the hybrid method should be constructed. This is done by identifying the best practices from the DSM- and OBIA-methods. The best practices of the methods are defined by the method-variant with the input and parameter settings resulting in the highest similarity relative to the validation dataset. The resulting hybrid method will be explained in chapter 5.5. The final research question is: *What improvement is realized by the hybrid method?* Chapter 5.6 will present a total comparison, in which the results of the hybrid method are compared to the results of the DSM- and OBIA-methods. A complete list of the absolute results of all methods relative to the validation dataset, with different parameter settings and inputs is presented in Appendix II. All deviations from the validation dataset are presented as similarity percentages to show how well each method variant performs. In Appendix III all absolute deviations from the validation dataset are presented, which are used to calculate the percentages.

5.1 DSM-Parameters

The DSM-method created by Alterra uses an AHN2 raster with a horizontal resolution of 50cm, so the default DSM-method uses that as well. The input AHN3 raster has been set to 50cm and 25cm to make the comparison with the OBIA-method that also uses those horizontal resolutions. The input variable is the AHN3 25cm for the different model parameters, because that is the most recent data with the highest resolution and therefore should return the results closest to the validation dataset. The neighbourhood, NDVI threshold and Roughness threshold are changed from the default model parameters to determine what their impact is on the results.

Next to the different input datasets and different resolutions that are tested, the tools that are used can use multiple operational parameters that will result in different outcomes for the model. Influential parameters that are used in the DSM-method are the NDVI-threshold, the roughness-threshold and the neighbourhood sizes of the peak determination phase. The model has been executed multiple times to compare the results for these different inputs. After comparing AHN2 with AHN3, it became clear that the AHN3 input data was more reliable with the best results at 25cm resolution. Therefore, the input parameters were tested for AHN3 at 25cm resolution as well. Table 1 shows the

different model parameters that were used as input for the different versions of the DSM-method using AHN3 at 25cm resolution. As shown, the input parameters were tested for each operation individually, while using the default parameters for the other operations.

Table 1: Input parameters for different DSM-method versions

Model Parameters	**Default**	**Large neighbourhoods**	**Small neighbourhoods**	**High NDVI**	**High Roughness**
Neighbourhood	4m	5m	3m	4m	4m
Neighbourhood	6m	7m	5m	6m	6m
NDVI	0.2	0.2	0.2	0.3	0.2
Roughness	0.2	0.2	0.2	0.2	250

The default neighbourhood radius setting in the DSM-method has been set at 4m for small trees and 6m for large trees. To see what the effects of the neighbourhood setting are the radius has been set to 1m larger and 1m smaller for both tree sizes. Clement (Meijer et al., 2015, p. 18) describes the process of selecting the neighbourhood settings as: *"In an iterative process corrections are made to the size of the zones"*. Therefore, to find what radius zones work best for the model, both a smaller and a larger neighbourhood setting have been executed. The default NDVI threshold is set at 0.2 in the Alterra method (Meijer et al., 2015, p. 20). As seen in the example in Figure 14 there are still objects that have been incorrectly passed the filtering process. Therefore, the NDVI threshold has been set at 0.3 to see if these objects can be filtered out. The threshold is not tested at 0.4 or higher, because then it could filter parts of the vegetation areas. The roughness threshold is set at 250, because as shown in Figure 26, the roughness at the edge of the tree crowns is around 250 and a higher threshold would exclude those pixels.

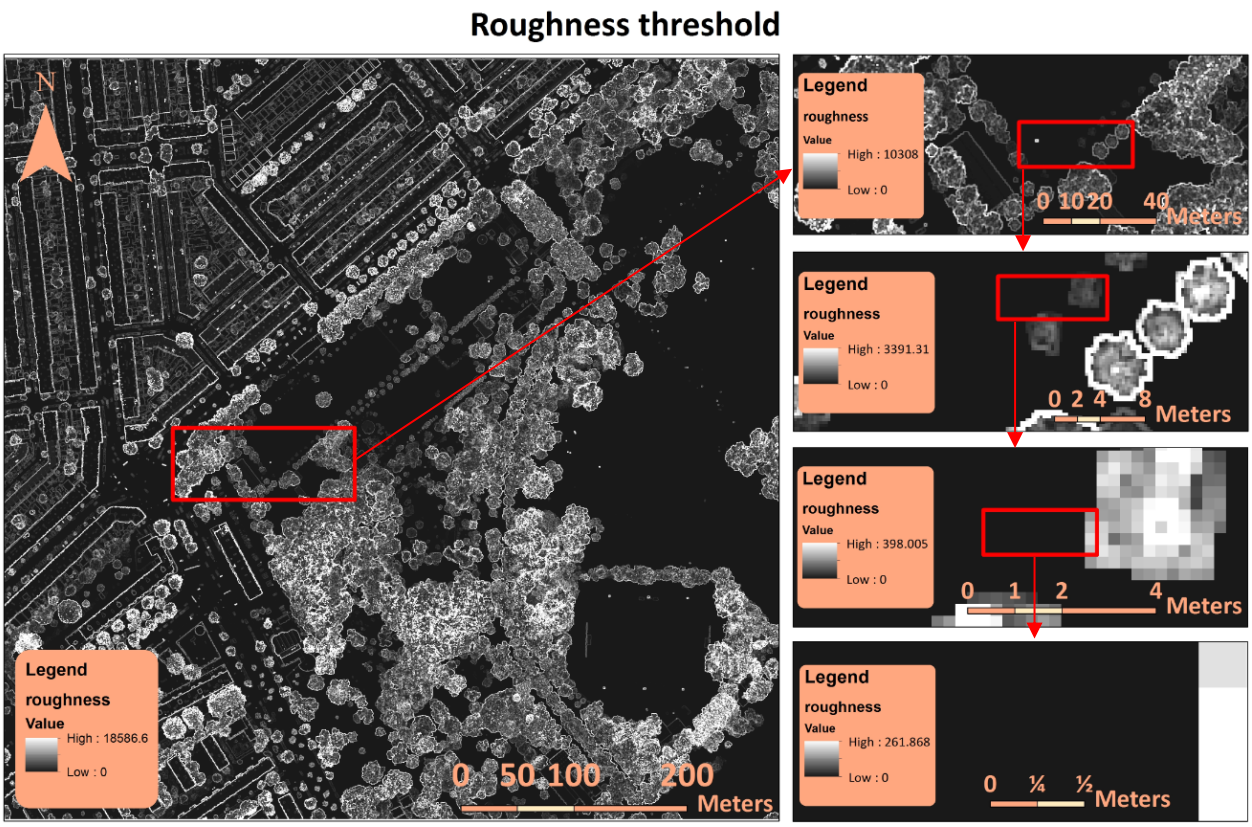

Figure 26: Roughness threshold

5.2 Validation results of the DSM-method

The results relative to the validation dataset are presented as similarity percentages. These are based on the deviations of individual trees as identified by each method as shown in chapter 2.5. The deviations from the validation set are summed up for the different tree type categories and are given a colour scheme ranging from green for the least total deviation from the validation set to red for the most total deviation from the validation set. This was done for all composition types and for both count and area deviations.

5.2.1 Single trees

Within the validation dataset there are 7 single trees identified. Therefore, a perfect count similarity percentage of 100% requires 7 trees to be identified by the method. If there are two trees identified by the method, where there is only 1 in the validation dataset, like in Figure 9, the count deviation is 1. When the same method doesn't identify another single tree, while there is one present in the validation dataset, the count deviation will be 2. In this example there will be 7 trees identified by the method, which corresponds to the validation data, but because the validation method uses deviations the similarity percentage will be 77.8% instead of 100%. The area similarity is calculated in a similar way, for

example: the area of the first single tree in the validation dataset is 251.55 m² and the area of the first single tree according to the default DSM-method is 189.75 m². This results in a count deviation of 61.80 m² for this tree.

Table 2: Results of the DSM-method for single trees

Single trees			
DSM	**Count similarity (n=7)**	**Area similarity (n=7)**	**Average similarity**
Default	87.5%	72.2%	79.8%
AHN3	87.5%	90.2%	88.9%
AHN3 25cm	87.5%	89.8%	88.7%
AHN3 large neighbourhood	87.5%	89.8%	88.7%
AHN3 small neighbourhood	58.3%	89.6%	74.0%
NDVI	100.0%	73.6%	86.8%
Roughness	77.8%	85.8%	81.8%

The results in Table 2 show that the Default DSM-method has 87.5% similarity to the validation dataset in the tree count, which is relatively close compared to the AHN3 version with the small neighbourhood parameter. As shown in Appendix II, a count similarity of 87.5% means that there is 1 tree deviation in the default DSM results, compared to the trees counted in the validation dataset. The variant that uses a different NDVI threshold has a 100% count similarity, meaning that 7 trees were counted, the same number as in the validation dataset. Contrary to the result in the count similarity, the NDVI variant has one of the largest deviations in the single tree areas, next to the default method. The variant that uses AHN3 at a 50cm resolution has the closest area similarity to the validation dataset. The AHN3 25cm input and the variant with the larger neighbourhood settings have the same results. The small neighbourhood settings show the largest count deviation from the validation dataset.

5.2.2 Rows of trees

The results for the rows of trees are divided into two tables. Table 3 shows the similarities to the validation dataset when the areas of tree crowns are counted as individual trees. Table 4 shows the similarities to the validation dataset when the areas of tree crowns are grouped together and the crown areas in the row are considered as one. The count similarities are the same for both tables, because the trees in a row are still counted as individuals in Table 4. This is the case in every method. When grouping the crowns of a row, the number of trees doesn't change. However, it is possible that the individual crown areas in the row show large deviations from the ones in the validation dataset, while the combined crown areas cover roughly the same area. This means that for the count similarity there are 17 individual trees taken into account. The area similarity that calculates the areas of trees in rows as

individually consists of 17 trees as well. These 17 trees are located in 3 different groups, which means that the area similarity of the rows in total is determined using 3 groups.

The results show that this distinction does influence the performance of a model variant. The results from the individual tree areas in a row have different variants that are relatively close to the validation dataset compared to the results from the total tree areas in a row. When considering the individual tree areas, the AHN3 of 50cm resolution is the closest DSM-variant to the validation dataset, while when considering the total tree areas, the AHN3 of 25cm resolution is the closest DSM-variant to the validation dataset.

Table 3: Results of the DSM-method for rows of trees as individuals

Rows of trees individual

DSM	Count similarity (n=17)	Area similarity (n=17)	Average similarity
Default	100.0%	77.5%	88.7%
AHN3	89.5%	80.4%	79.1%
AHN3 25cm	100.0%	75.8%	87.9%
AHN3 large neighbourhood	100.0%	72.3%	86.1%
AHN3 small neighbourhood	100.0%	80.0%	90.0%
NDVI	89.5%	71.4%	74.6%
Roughness	100.0%	72.9%	86.5%

Table 4: Results of the DSM-method for rows of trees total

Rows of trees total

DSM	Count similarity (n=17)	Area similarity (n=3)	Average similarity
Default	100.0%	79.6%	89.8%
AHN3	89.5%	83.2%	80.5%
AHN3 25cm	100.0%	90.0%	95.0%
AHN3 large neighbourhood	100.0%	76.4%	88.2%
AHN3 small neighbourhood	100.0%	84.8%	92.4%
NDVI	89.5%	79.9%	78.9%
Roughness	100.0%	82.2%	91.1%

The similarities to the validation set are smaller when using the individual tree areas, than when using the total area in all DSM variants. When tree crowns in a row are considered as individuals, the AHN3 with a small neighbourhood has the closest average similarity percentage, while for the total tree crows in a row, the variant that uses the AHN3 at 25cm and the default neighbourhood settings has the highest average similarity percentage. Both tables have the variant with the higher NDVI threshold as the lowest average similarity percentage.

5.2.3 Groups of trees

For the groups of trees, the crown areas of all trees in a group are considered as part of the group and are not considered as individual crowns. As shown in Appendix I there are 4 groups of trees validated, with two groups consisting of 3 trees and the other two groups consisting of 6 trees, of which one is shown in Figure 10Figure 10: Example of a count deviation of 4 for a group of trees. It was not possible to take larger groups into account, because the manual validation method proved to be unreliable when many trees were in close proximity.

Table 5: Results of the DSM-method for groups of trees

Groups of trees

DSM	Count similarity (n=18)	Area similarity (n=4)	Average similarity
Default	75.0%	78.2%	76.6%
AHN3	78.3%	86.2%	82.2%
AHN3 25cm	75.0%	90.7%	82.8%
AHN3 large neighbourhood	69.2%	89.2%	79.2%
AHN3 small neighbourhood	75.0%	90.3%	82.7%
NDVI	72.0%	87.7%	79.8%
Roughness	75.0%	89.6%	82.3%

The results for the groups of trees in Table 5 show that the counts of all variants have a relatively larger deviation from the validation dataset compared to the results in the rows. The variant with the closest similarity to the validation set is the one that uses the AHN3 at 50cm resolution as input. The areas of the datasets using the AHN3 at 25cm resolution as input are the closest to the validation in terms of area similarity. For the average similarities, the variant using the AHN3 25cm resolution, combined with either the default or small neighbourhood settings, are closest to the validation set. The AHN2 default variant shows the largest area deviation from the validation dataset, resulting in the lowest average similarity percentage.

5.3 OBIA-Parameters

The default OBIA-method is constructed based on the method developed by Davids (2013). The tool that is crucial to the OBIA-method is the multiresolution segmentation algorithm. Small differences in parameter settings determine the shape of the individual segments, which influence the results. Therefore, the tested variables for the OBIA-method are parameters of the multiresolution segmentation tool. To make a comparison with the default DSM-method using AHN2 at 50cm resolution, the OBIA-method was tested using a 50cm resolution AHN3, as well as a 50cm resolution AHN2. In Table 6 the different input parameters are presented.

Table 6: Input parameters for different OBIA-method versions

Model Parameters	Default	Weights	Scale parameter	Shape	Compactness
Weight NDVI	5	10	5	5	5
Weight returns	10	5	10	10	10
Weight elevation	10	5	10	10	10
Scale parameter	5	5	10	5	5
Shape	0.1	0.1	0.1	0.5	0.1
Compactness	0.5	0.5	0.5	0.5	1

The default settings of the multiresolution segmentation tool have a scale parameter threshold of 5, the shape value of 0.1 and the compactness value of 0.5. As shown in Figure 21, the scale parameter sets the maximum standard deviation of the homogeneity criteria (Wageningen University, 2014). This defines the threshold where the object growth stops if it is exceeded, so a larger scale parameter will result in larger objects (Yan, 2003, p. 17). The Shape is the smoothness + compactness (Wageningen University, 2014), so if the shape is relatively high and the compactness stays the same, the smoothness will be high as well. If the shape stays the same as the default, but the compactness increases the smoothness will be relatively low.

The segmentation is executed with a scale parameter value of 10, to create large homogeneous objects, excluding smaller areas from the classification (Yan, 2003, p. 56). A change in scale parameter causes a different tree crown shape, because pixels are segmented into relatively larger objects. This means that there are more pixels with a NDVI value in a segment, resulting in less extreme differences in average NDVI. The segments which now pass or don't pass the average NDVI classification threshold will be bigger. This causes the shape of the tree crown to be different compared to having the scale parameter set at the default. The variants of the multiresolution segmentation with a different shape value of 0.5 and a compactness value of 1 are used to obtain the parameters most suitable for identifying trees. In the default multiresolution segmentation, the number of returns and the elevation are given the highest weight. Elevation and number of returns are indicators whether an object is a tree or part of other vegetation types, especially in areas with high vegetation variance like parks. The NDVI is a better indicator in urban areas, because trees can have similar elevation values as buildings and other

human made objects. Therefore, the multiresolution segmentation is executed with NDVI as highest weight as well.

5.4 Validation results of the OBIA-method

The default variant of the OBIA-method uses the AHN3 25cm resolution as input. The AHN3 at 50cm resolution and the AHN2 at 50cm resolution inputs are used as well to compare the results to the DSM-method. The model was executed with different inputs, different weights, with another scale parameter, with a different shape parameter and with another compactness parameter. The results of the OBIA-method with different inputs and parameters are compared to the same validation dataset as the results of the DSM-method.

5.4.1 Single trees

Table 7: Results of the OBIA-method for single trees

	Single trees		
OBIA	**Count similarity (n=7)**	**Area similarity (n=7)**	**Average similarity**
Default	100.0%	91.6%	95.8%
CellSize	100.0%	89.4%	94.7%
AHN2	100.0%	77.1%	88.6%
Weights	100.0%	93.0%	96.5%
ScaleParameter	100.0%	89.6%	94.8%
Shape	100.0%	93.5%	96.7%
Compactness	100.0%	92.0%	96.0%

The results for the single trees as shown in Table 7 show that none of the variants have a count deviation from the validation dataset. Almost all the calculated crown areas look close to the validation dataset as well, however the variant that uses AHN2 as input is a clear outlier that has an area similarity more than 10% lower to the validation dataset than the next lowest variant.

5.4.2 Rows of trees

As explained in chapter 5.2.2, the count similarity percentage is the same in Table 8, where the individual tree areas in the rows are calculated, as in Table 9, where the areas are grouped per row. What stands out when looking at the count, is that the variant that uses the AHN2 has a large deviation from the validation dataset. When looking at the area similarity of the AHN2 variant, the deviation is also large for the individual trees in the row, but the deviation is relatively small when looking at the tree areas

grouped together. The default OBIA-method has the closest area similarity when the tree areas are merged, while the similarity is average when they are considered as individual areas. For the variant that uses a higher compactness parameter, the opposite is true. Overall, all areas are closer to the validation dataset when the trees are considered as a group than when they are considered as individuals.

Table 8: Results of the OBIA-method for rows of trees as individuals

Rows of trees individual

OBIA	Count similarity (n=17)	Area similarity (n=17)	Average similarity
Default	100.0%	72.6%	86.3%
CellSize	100.0%	68.0%	84.0%
AHN2	77.3%	63.9%	70.6%
Weights	94.4%	77.8%	86.1%
ScaleParameter	89.5%	76.4%	82.9%
Shape	94.4%	76.2%	85.3%
Compactness	100.0%	79.1%	89.6%

Table 9: Results of the OBIA-method for rows of trees total

Rows of trees total

OBIA	Count similarity (n=17)	Area similarity (n=3)	Average similarity
Default	100.0%	94.9%	97.5%
CellSize	100.0%	79.9%	90.0%
AHN2	77.3%	89.7%	83.5%
Weights	94.4%	86.6%	90.5%
ScaleParameter	89.5%	89.6%	89.5%
Shape	94.4%	90.6%	92.5%
Compactness	100.0%	87.9%	94.0%

5.4.3 Groups of trees

Table 10: Results of the OBIA-method for groups of trees

Groups of trees			
OBIA	**Count similarity (n=18)**	**Area similarity (n=4)**	**Average similarity**
Default	75.0%	90.3%	82.7%
CellSize	69.2%	93.3%	81.2%
AHN2	72.0%	87.9%	80.0%
Weights	66.7%	87.4%	77.0%
ScaleParameter	72.0%	90.2%	81.1%
Shape	69.2%	88.6%	78.9%
Compactness	66.7%	87.1%	76.9%

The results for the groups of trees of the OBIA-method in Table 10 show a low count similarity compared to the results of the single trees and to the rows of trees. There are no particularly large outliers identified in the count similarities, with the default method having the closest results to the validation dataset. The area similarities are relatively high overall, with the variant that uses the AHN3 with a cell size of 50cm having the closest total crown area for 93.3% identical to the validation dataset. In all previous results for the OBIA-method, the variant using the AHN3 with a resolution of 25cm has a higher similarity percentage. Another interesting result is that the variant that uses the higher compactness parameter has the lowest average similarity for the groups of trees, while it had the highest average similarity for the rows of trees as individuals. The variant that uses the different weights for the segmentation has a high deviation from the validation dataset as well.

5.5 Constructing the Hybrid method

The final research objective of the thesis was to create a new method that is based on the best practices of the DSM- and OBIA-methods. The hybrid method is based on the multiresolution segmentation and individual tree delineation techniques from the OBIA-method. The new method uses the filters from the DSM-method to exclude the pixels that are below a certain NDVI, elevation and roughness threshold to be considered trees, such as buildings and water before executing the segmentation analysis.

5.5.1 Best practices

The best practices are identified by comparing the different results of the input parameters and variables in the DSM and OBIA-method. For both methods, the variant that has the highest average similarity percentage is the one that has the AHN3 at a resolution of 25cm as input and uses the default parameter settings. Therefore, the default parameter settings and AHN3 are used for the combined method as well.

From both methods, the operations that were considered most suitable for identifying tree crowns were chosen to be used in the new method. The shapes of the individual crowns are decided by the delineation operations. The DSM-method uses the Euclidean distance to determine the border of crowns between peaks, which results in pixels being assigned to a peak based on the closest distance. The OBIA-method uses the growth algorithm, which results in segments being assigned to a peak based on the largest boundary of the neighbouring segments. In Figure 25 an example of this process is shown. In Figure 9 an example is shown of the delineation in the DSM-method based on the Euclidean distance between two tree crowns. From this visual comparison, it becomes clear that using the growth algorithm results in a more natural border between the different assigned peak areas compared to using the Euclidean distance. Therefore, the combined method uses the growth algorithm to delineate the individual crowns.

The growth algorithm is using the different tree segments and the identified peaks as input. The identification of the peaks is done in the same way for both the DSM- as the OBIA-method by comparing the highest elevation pixels with their neighbourhood. The DSM-variant that uses the default neighbourhood settings have the highest average similarity percentage to the validation dataset, so the default settings are used in the combined method as well. For the multiresolution segmentation, the OBIA-variant that uses the default parameter settings has the highest average similarity percentage, so for this operation the default parameter settings are used as well. To include operations from the DSM-method and create a new, combined method, the filters of the DSM-method have been applied before executing the multiresolution segmentation. The use of filters will lead to a higher correctness of the results, where more objects that could be incorrectly classified as trees are excluded from the dataset (Meijer et al., 2015, p. 61). The filter is based on the default NDVI and roughness threshold and is applied to the AHN3 dataset, in the pre-processing phase to exclude the filtered areas from the pointcloud in LAStools. Figure 27 shows the segmentation result for a single tree with a NDVI grey scale background after the filters from the DSM-method have been applied.

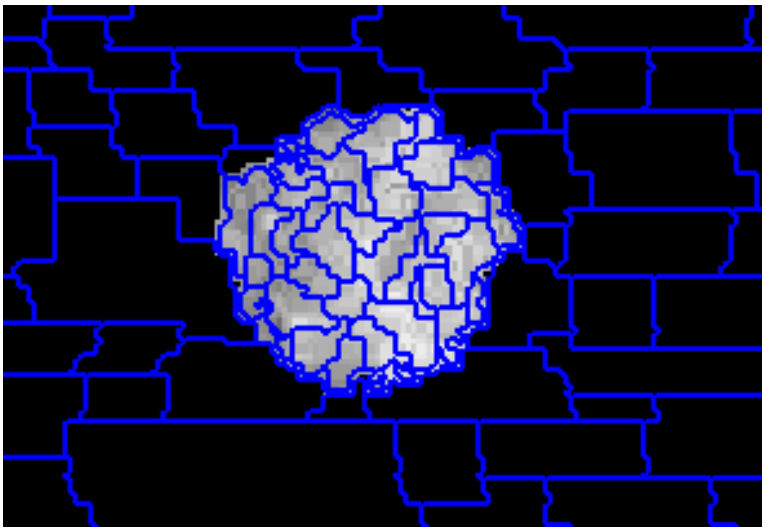

Figure 27: The result of multiresolution segmentation for the hybrid method

As a result of applying the filters on the pointcloud, the pre-processing in eCognition had to be changed as well. The default interpolation operation as used in the OBIA-method before the multiresolution segmentation, could not be applied on the combined method. The filters were used to exclude the areas in the pointcloud and other input datasets that were above the filter thresholds, so as seen in the left side of the map in Figure 14, a large part of the study area now doesn't include any data. As a result, the default interpolation algorithm could not be applied, because there were too many pixels with no data. Within eCognition, it is not possible to save the intermediate results of the interpolation loop, causing the computer memory to overload and crash. Therefore, the interpolation pre-processing was only executed in three cycles to fill the gaps in the tree crowns that are a result of a too low point density in certain areas.

5.5.2 Results of the hybrid method

In the hybrid method, only one variant is created, which is based on the filters that are created in the DSM-method before applying the multiresolution segmentation technique. This way, elements of both methods are used with the aim to create a new and improved method. The results in Table 11 are presented differently than the results of the DSM- and OBIA-methods. There is only one variant so it wouldn't make sense to split the results into multiple tables. The results in this table are presented for all tree composition types, with the colours scaled from red to green between the different composition results instead of the model variants in the DSM- and OBIA-methods.

Table 11: Results of the hybrid method

Hybrid method	Count similarity	Area similarity	Average similarity
Single trees	100.0%	94.3%	97.2%
Rows of trees individual	85.0%	78.9%	82.0%
Rows of trees total	85.0%	95.2%	90.1%
Groups of trees	72.0%	88.6%	80.3%

The results of the hybrid method show that for single trees, the count similarity is 100% and the area similarity is with 94.3% close or the validation dataset as well. In this table, it is also clear to see that there is a large difference in area similarity if taking rows as individuals compared to considering the crowns of rows as a group. This has been the case in all previous variants for both methods, but because in this table all tree composition types are compared, this contrast is more obvious. The relatively low count similarity for the groups of trees is also better highlighted in this table, because the count similarity is generally lower in the groups compared to the other composition types.

5.6 Total Comparison

In this final subchapter of the results, the the total comparison will be highlighted. In the total comparison, all tree composition types are comparison, all tree composition types are combined to see what the overall results are for the methods. The results have been split into two The results have been split into two categories, with one taking the rows of trees as individual crown areas into account and the other the areas into account and the other the combined crown areas of the rows.

shows the results of the different tree composition types combined for all tested methods. There are two different columns for the sum of all areas, one which includes the trees in rows as individual trees and one which includes the trees in rows as a combined area. This was not necessary for the count similarities, because these stay the same for both row-area variations. As in the previous tables, the results are coloured by columns, where the results that are closest to the validation dataset are green and the results that are furthest from the validation dataset are red.

Table 12: Overview of total similarities for all methods

Total similarities

	Count	**Area**	**Area**	**Average**	**Average**

	similarity (n=42)	similarity individuals in rows (n=28)	similarity grouped rows (n=14)	similarity individuals in rows	similarity grouped rows
DSM Default	85.7%	76.8%	77.6%	81.2%	81.7%
DSM AHN3	84.0%	84.3%	85.6%	84.1%	84.8%
DSM AHN3 25cm	85.7%	83.7%	90.3%	84.7%	88.0%
DSM AHN3 la neighbour	82.4%	81.4%	83.5%	81.9%	82.9%
DSM AHN3 sm neighbour	79.2%	85.6%	87.8%	82.4%	83.5%
DSM NDVI	82.4%	77.7%	81.7%	80.0%	82.0%
DSM roughness	84.0%	81.3%	85.7%	82.6%	84.9%
OBIA Default	87.5%	82.2%	92.4%	84.8%	90.0%
OBIA CellSize	84.0%	80.3%	86.6%	82.1%	85.3%
OBIA AHN2	77.8%	74.4%	86.5%	76.1%	82.1%
OBIA Weights	80.8%	84.0%	88.0%	82.4%	84.4%
OBIA ScaleParameter	82.4%	83.8%	89.8%	83.1%	86.1%
OBIA Shape	82.4%	83.7%	90.3%	83.0%	86.3%
OBIA Compactness	82.4%	84.4%	88.3%	83.4%	85.3%
Hybrid method	80.8%	85.1%	92.2%	83.0%	86.5%

Looking at the count similarities, the OBIA-method that uses the AHN2 as input has a similarity of 77.8% and therefore the largest deviation from the validation set. Interestingly the default DSM- and default OBIA-method have the highest similarity for each respective method, with the OBIA default having the overall highest count similarity of all variants. In the DSM-method, the AHN3 25cm variant has a high count similarity as well, while the variant that uses a small neighbourhood has a low similarity. In the OBIA-method, the AHN2 variant has the lowest count similarity compared to the validation dataset. The count similarity of the hybrid method is relatively low compared to the other methods.

For the area similarity when considering row areas as individuals, the DSM-method with a small neighbourhood has the highest percentage, followed by the hybrid method. Both the DSM- and the OBIA-method variants that use the AHN2 as input have the lowest similarity percentages. When the areas in the rows are grouped, the results of the default OBIA-method have the highest area similarity percentage of 92.4%. The hybrid method has a high percentage as well with 92.2%. For both the DSM- and OBIA-methods, the variant that uses the AHN2 as input has the lowest similarity. In the DSM-method the default parameters with the AHN3 25cm resolution input has the highest similarity percentage.

When averaging the scores, the distinction between the different row-area variations has been made as well, resulting in two different average columns. By averaging the scores it can be determined what the most suitable method is when count and area of tree crowns are equalliy important. In all methods, the average percentages are higher when combining the tree row crowns areas. In both columns, the default OBIA-method has the highest average similarity percentage, respectively 84.8% and 90.0%. Therefore, the default OBIA-method is closest to the validation dataset if both crown count and crown area are equally important. For the DSM-method, the variant that uses the AHN3 at 25cm resolution and the default parameters has the highest average percentages, respectively 84.7% and 88.0%. The average similarity results from the hybrid method are with 83.0% and 86.5% close to the validation dataset, however the percentages are relatively low compared to the highest similarity results in both the DSM- and OBIA-method.

6. Conclusion & Discussion

In this final chapter, the first part will be a conclusion based on the results. The second part is the discussion of the results and methods where interesting observations will be highlighted and limitations of the methods will be stated. The final part consists of recommendations, based on the discussion and conclusion. Furthermore, potential implementations of the crown identification and suggestions for future improvements will be presented.

6.1 Conclusion

The general objective of this thesis was to to develop a new, improved method to identify individual tree crowns. To realize the objective, first the DSM- and OBIA-methods were analysed to determine how they identify individual tree crowns. The hybrid method is constructed based on the best practices of the DSM- and OBIA-method. The first research question is: *How can the DSM- and OBIA-methods be compared for identifying individual trees?* This question is answered by reviewing the processing steps that are taken and by comparing the performance for different tree compositions when using different input datasets and model parameters. This comparison is used to define the best practices that are used to create the hybrid method, which is a combination of the most suitable tools for tree crown identification identified from both DSM- and OBIA-methods. The best practices of the DSM- and OBIA-methods are used to answer the second research question: *How should the hybrid method be constructed?*

For both methods, it can be concluded that the performance increases when using a 25cm resolution elevation model, instead of one that has a resolution of 50cm. For both methods, the results of the variant that uses the AHN3 as input are closer to the validation dataset than the variant that uses the AHN2. However, this cannot be fully attributed to the difference in point density or between the two datasets, because the date when the validation data was acquired is closer to the date of the AHN3 than it is to the date of the AHN2. Therefore, it is not possible to conclusively state that the AHN3 is more suitable for identifying tree crowns in all scenarios. For both the DSM- and the OBIA method, the variant that uses the default parameters is closest to the validation dataset.

For identifying individual tree crowns, the results have shown that single trees are more easily identified than rows and groups. Especially in groups there is often a larger count deviation. When looking at the crown areas, the individual trees within groups with a large count deviation like shown in Figure 10 are impossible to calculate. Therefore, these areas are combined to compare the overall group area similarities. For trees in rows, both the areas of individual crowns as the combined areas are taken into account. All variants that were executed have a higher similarity percentage when comparing the crown areas than when they are calculated as individuals. This was expected, because if one tree in the row has a larger crown area than the tree in the validation dataset and another tree has a smaller crown area, the total deviations are summed up. When using the combined crown areas, these deviations disappear if they are between the individual crowns within the row. The average similarity percentage to the total validation dataset is the highest for the default OBIA-method. However, the difference in

similarity percentage between the DSM- and OBIA method is small, so the OBIA-method is slightly more suitable for identifying individual tree crowns.

The final research question is: *What improvement is realized by the hybrid method?* By answering this question it is possible to determine if the objective of this thesis is achieved. The total area similarity percentages of all trees in Table 12 show that the hybrid method has a high similarity percentage relative to the validation dataset. This is the case when trees in rows are viewed as individuals as well as when the tree areas in rows are combined. However, when tree areas in rows are considered individuals, the DSM-variant that uses a small neighbourhood is closer to the validation dataset. When tree areas in rows are combined, the default OBIA-variant is closer to the validation dataset. Both of these variants have a relatively low similarity percentage in the other categorie. This means that using one of these variants are best suitable when it is clear whether trees in rows should be regarded as individuals or should be combined. When this is not clear beforehand, the hybrid method is the best option, because it gives a close result to the validation dataset either way.

When looking at the count similarity in Table 12, the hybrid method has a relatively low similarity to the validation dataset. Therefore, when the objective is to find the number of individual trees in an area, the hybrid method is less suitable compared to the default DSM- and OBIA-methods. In this case, the default OBIA-method has the best results compared to the validation dataset. Finally, the results for the tree composition types will indicate what method is most suitable when only one composition type is relevant. For single trees, the hybrid method has the highest average area similarity percentage relative to the validation dataset and has a count similarity of 100% as well. Therefore, the hybrid method is the best suitable method for identifying single trees. When considering the area of trees in rows individually, the hybrid method has a relatively high area similarity percentage, however there are several variants of the DSM- and OBIA-methods that perform better. The count similarity of the hybrid method is low, so when looking at individual tree crowns within rows, no improvement is realized by the hybrid method .

If the areas of trees in rows are combined, the hybrid method has the highest similarity percentage. However, because the count similarity is relatively low, it is more suitable to use the default OBIA-method when both area and count should be taken into account. For trees in groups, neither the combined area similarity, nor the individual tree count similarity is improved by the hybrid method. In this case both the default OBIA-method and the DSM-method that uses the AHN3 with a resolution of 25cm are best suitable. It depends on what somebody wants to achieve with the crown identification method to determine whether the hybrid method is an improvement. It is not possible to conclude that the hybrid method is an overall improvement compared to the DSM- and OBIA-methods. In most cases, the hybrid method is more suitable for crown area estimation, but less suitable for crown count estimation.

6.2 Discussion

The discussion chapter consists of an explanation of the results of all methods, both individually as well as in relation to each other. In each subchapter, the limitations of the methods that have influenced the results will be discussed as well. Next to the influences of the limitations within the different tree crown identification methods, there are flaws in the validation method that also need to be discussed. Overall, the discussion will highlight the findings of all methods based on a reflection on the research objectives and findings in the literature.

6.2.1 DSM-method

The first step in reviewing the DSM-method was to identify the processing steps. The model algorithm was developed for Alterra by Jan Clement and has a report that describes the general processing procedures (Meijer et al., 2015). In Figure 28 the flowchart of the crown extraction algorithm shows an overview of this method. However, the report of Alterra is not always clear on how certain operations were carried out, and they state that some parameters and operations were chosen based on an iterative process where the intermediate results were visualised and rated for their application possibilities (Meijer et al., 2015). The final choices of the parameters that were used are not presented in the report.

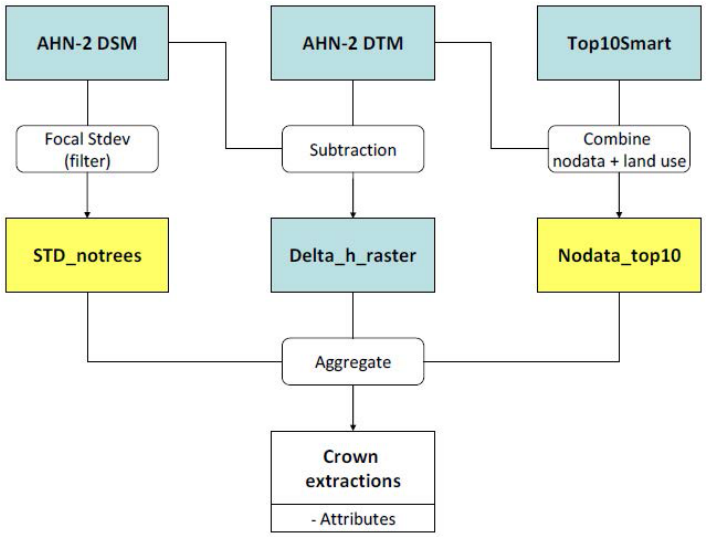

Figure 28: Flowchart of the crown extraction algorithm developed by Alterra (Meijer et al., 2015, p.16)

Therefore, it was not possible to fully develop the exact default method as developed by Alterra, which means that it is possible that the final parameter settings used for the default algorithm in this study are slightly different from the model developed by Jan Clement. Overall the same procedure is taken, which first defines the filters, secondly the peaks and thirdly the crown extraction.

In terms of the tree count similarity to the validation dataset, it is interesting that the default method performs better at rows of trees than at single trees. The similarity to the groups of trees is the lowest, which is expected, because there is usually a less clear transition in height between the different crowns in a group than between the trees in a row if the species are the same. The trees in rows are more often of the same species, however in this study area the trees in groups are standing closer together making it more difficult for the algorithm to distinguish them. Interestingly, this doesn't show at all from the area similarities in the default DSM-method, where the single trees have a lower similarity percentage than the rows and groups. This can be explained by the fact that the default method uses the AHN2 from 2008 as input, while the only available CIR aerial image that was used to create the NDVI filter is from 2016.

Due to the temporal differences in the different input datasets it was expected that the method performs better using the AHN3. All model variants are using the same NDVI filter from 2016, while AHN2 is from 2008 and AHN3 is from 2014. Therefore, the AHN2 results are more likely to be influenced by this difference in environmental changes over time than the AHN3 results. The method developed by Clement does use an image from 2008 to calculate the NDVI (Meijer et al., 2015, p. 19). The results for the default AHN2 image with 0.5m resolution in this thesis were expected to be less accurate than the results from Alterra, because Alterra uses a NDVI from the same year as the AHN2. The method developed by Clement has a maximum crown area completeness of 77.8% (Meijer et al., 2015, p. 62). In this study, the highest total crown area similarity calculated in the variants using the default parameters of the DSM-model is 90.3%.

Figure 29: Crown validation as used by Alterra (Meijer et al., 2015, p. 33)

This could be explained by the differences in final parameter settings. In Figure 29 the validation method of Alterra is shown, where red delineations represent the reference dataset and green delineations the model output (Meijer et al., 2015, p. 33). This validation method clearly differs from the one used in this study, which will have influenced the crown similarity results as well.

Regarding the performance of the DSM-method in this study when using different input sources, the area similarity is closer to the validation dataset when using the AHN3 than it is using the AHN2. Interestingly, when looking at tree crowns individually for the single trees and rows, the variant using the AHN3 at 50cm resolution as input performs best. When combining the crown areas for the rows and groups, the variant using the AHN3 at 25cm resolution as input performs best. The count similarities between the three variants are identical for single trees, in the rows the AHN2 and AHN3 at 50cm are identical to the validation dataset, but for the groups the AHN3 at 25cm performs best. It is not possible to determine what input dataset for the DSM-method is most suitable overall for the crown count overall, based on these results. In the overview of the total similarities as shown in Table 12, the variant that uses the AHN3 at 25cm resolution as input has the highest average similarity to the reference dataset.

All variants with different model parameters are using the 25cm resolution AHN3 as input and are executed with 1 different parameter setting form the default model. The results show that for none of the tree composition types, the variant that uses a larger neighbourhood has a higher count or area similarity percentage than the variant using the default parameters. A large neighbourhood means that the algorithm uses a larger radius to identify peaks, resulting in fewer peaks in total. This reduces the count of the crown areas and increases their size. When using a smaller neighbourhood, the opposite is true, so more peaks are identified, leading to a higher count and a smaller crown size.

The variant that uses a higher NDVI threshold has a lower area similarity percentage than the default inputs in all tree compositions. The high threshold will have caused fewer pixels to be identified as part of a crown, making the areas smaller compared to the validation dataset. However, when looking at the count, the smaller crown area resulted in a higher similarity percentage for single trees. When looking at Figure 9: Example of a count deviation of 1 for a single treeFigure 9, the count deviation of 1 can be explained by the peak identification method finding 2 peaks in the area. If the crown area is smaller, the algorithm would have only found 1 peak in the area resulting in the better count similarity for the variant using the higher NDVI threshold filter. This also explains the low count similarity of the variant that uses the small neighbourhood settings, because in that case the area of the crown stays the same, but there are more peaks identified within that area, resulting in the scenario of Figure 9 happening more often. Finally, the variant that uses a higher roughness filter threshold never performs better than the method using the default parameter settings. The higher roughness has caused the crown sizes to be smaller, resulting in a lower area similarity. A potential benefit of using a higher roughness threshold is that it filters out more objects that could incorrectly be classified as trees such as roofs on buildings or fields of grass. In this study, both those objects have been filtered out by the NDVI, building or elevation filter.

6.2.2 OBIA-method

Unlike the DSM-method, it was not possible to identify the OBIA-processing steps based on a single report. In this study, the segmentation method described by Davids (2013) was used in combination with a growth algorithm similar to that from the Boombasis (Wigger Tims, personal communication, March 7, 2017). A complete description of the method used for the Boombasis was not available, so it was not

possible to directly compare the method developed by NEO to the method developed by Alterra. This growth algorithm, as explained in Figure 25, merges the objects around the identified peaks based on the Eliminate and Merge tools in ArcMap. The peaks are identified in the same way as in the DSM-method, but instead of being based on single pixels, they are calculated using the resulting segments of the multiresolution segmentation technique.

Before the results of the different input parameters are discussed, the results of the default OBIA-method at different tree compositions will be evaluated, which is using the AHN3 pointcloud as input, converted to a raster with a horizontal resolution of 25cm. When looking at the crown count for the different compositions, the single trees and trees in a row have a 100% similarity relative to the validation dataset. The groups of trees on the other hand only have a 75% similarity percentage. This is likely due to the peak identification, of which the neighbourhood settings could have been too large. This results in a lower number of individual crowns being identified, like the example in Figure 10. The single trees, and usually the trees in rows as well, are standing further apart, so these have been distinguished better. The crown area similarity of the default method is the closest to the validation set for the rows of which the areas are combined. When the crown areas in rows are calculated as individuals, the similarity percentage is by far the lowest for all composition types. This means that the crown areas for rows are identified relatively well, however the distinction between the individual trees in rows is problematic. The count similarity for the rows is 100%, therefore it is likely that the peak identification went well, however the growth algorithm has merged a lot of segments to the wrong peaks. These segments are created by the multiresolution segmentation, so either the growth algorithm, or the default parameter settings are not ideal for identifying the crown areas of individual trees in a row.

In the OBIA-method the different input datasets that are used are the AHN3 and AHN2 pointclouds. The AHN3 pointcloud is converted to an elevation raster of 25cm and to an elevation raster of 50cm. The AHN2 is only used as a 50cm resolution raster, because a 25cm resolution raster is not used in the DSM-method. Furthermore, the AHN2 has fewer points per meter, so it is less reliable compared to the AHN3. When looking at the results of the crown count, the variant that uses the 50cm AHN3 raster has a 100% similarity to the validation dataset in the single trees and rows, similar to the default that uses the 25cm AHN3. It performs slightly worse for the group of trees. The variant that uses the AHN2 as input also has a 100% count similarity for single trees, but performs a lot worse for rows. Interestingly, the AHN2 variant does perform slightly better than the version that uses the AHN3 at 50cm for groups of trees, but still not as good as the 25cm default. The low count similarity in rows of the variant that uses the AHN2 can be caused by the poor area similarity of individual trees. When looking at the raw data in Appendix II, there are a lot of trees that are not identified due to the same effect as shown in Figure 10, which is caused by a low number of identified peaks. In Figure 30 an example of a row with a low count similarity is shown. In this figure, there are 6 validation trees, visualized by a green delineation. There are only two trees identified by the OBIA-method using the AHN2 as input, visualized in red and blue. The area similarity percentage is highest for the default OBIA-method in single trees and rows, but for groups the variant that uses the AHN3 at 50cm performs slightly better.

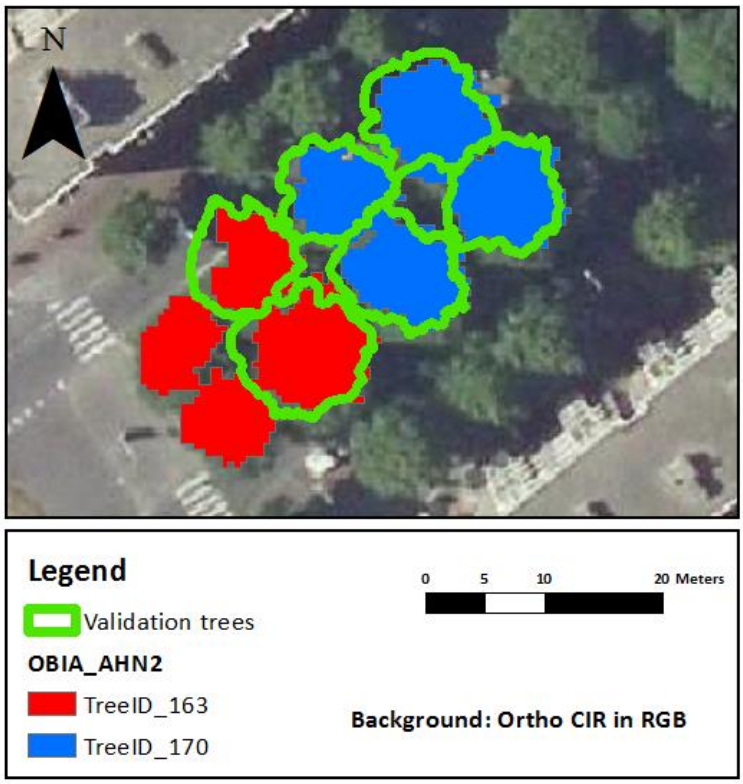

Figure 30: Example of count deviations caused by low number of identified peaks

The different input parameters are all executed using the AHN3 25cm resolution as input, because the average similarity percentage is highest in the default variant for all tree composition types. The first variant that will be discussed has used different weights for the multiresolution segmentation input data. In this variant, the NDVI has a relatively higher weight than the number of returns and the elevation. It was expected that the NDVI is a better tree indicator in urban areas compared to the park area, because the contrast in NDVI values between trees and their environment is higher. The results of this variant show that the different weights are more suitable to identify individual crown areas compared to the default dataset, but perform worse when identifying the areas of groups. This was expected, because the groups are standing closer together compared to single trees. Therefore, the NDVI contrast of a tree with its environment is larger for single trees than it is for groups.

The variant that uses a high scale parameter is causing the different segments to be larger in size. This results in a different final shape of the trees when applying the growth algorithm. The results show that this leads to a lower average similarity percentage compared to the default OBIA-parameters in all tree composition types. The large segments are causing a lower count similarity, because more segments are covering parts of multiple trees, due to the larger homogeneity threshold narrowing down the differences between the trees in the segmentation. The variant that uses a larger shape causes the smoothness of the borders of segments to increase and the compactness to decrease relative to the smoothness. In Figure 31 the difference is shown in segmentation results between one variant using a

shape parameter of 0.1 and a compactness parameter of 0.5 on the left side of the figure and another variant using a shape parameter of 0.9 and a compactness parameter of 0.5 on the right side (Wageningen University, 2014). In this comparison, it is visible that using a higher shape parameter results in a smoother border structure of the segments and the segments being large, because the compactness decreases relatively. In this study, the parameter was set to 0.5 instead of 0.9 to make this effect less extreme.

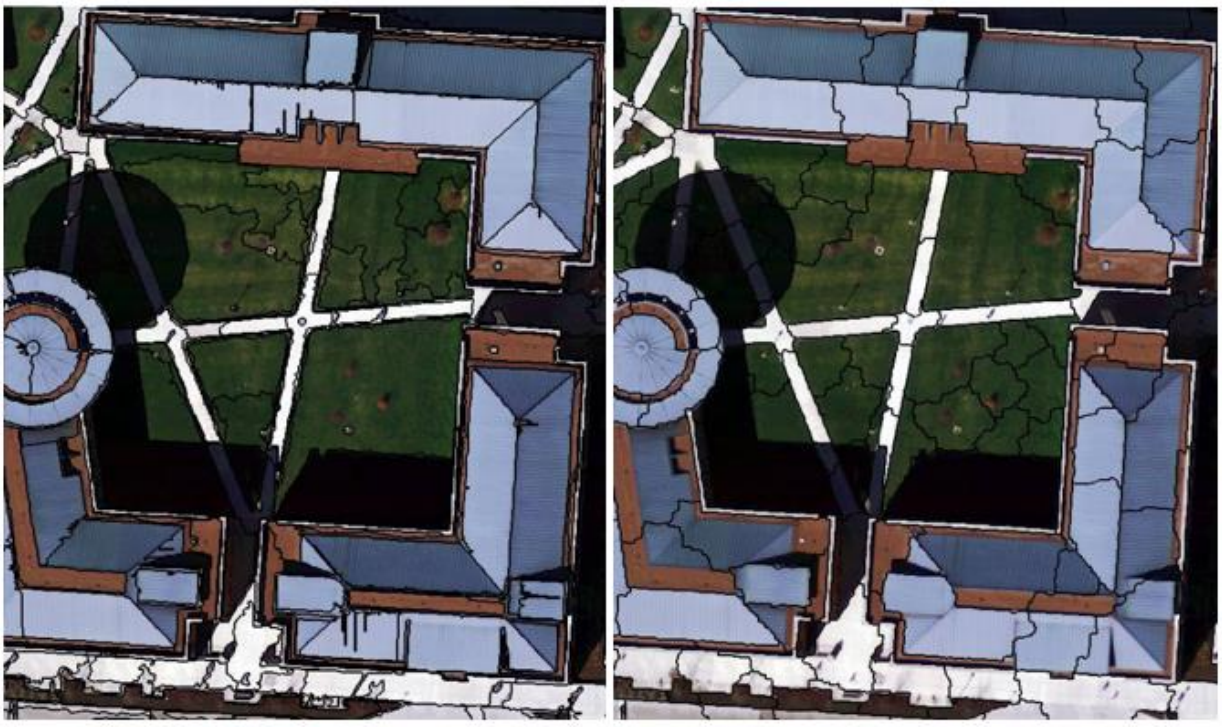

Figure 31: The effects of a higher shape relative to compactness in multiresolution segmentation (Wageningen University, 2014)

The results of the variant with the large shape parameter show that when identifying single tree crowns the area similarity percentage is very close to the validation dataset. However, when identifying the total crown areas for groups, the high shape parameter causes the area similarity percentages to be lower than the default. Interestingly, this is the case for the variant that uses the higher compactness parameter as well. In Figure 32 the results of the variant that uses the high compactness parameter is visually compared to the variant that uses the high shape parameter for a group of trees.

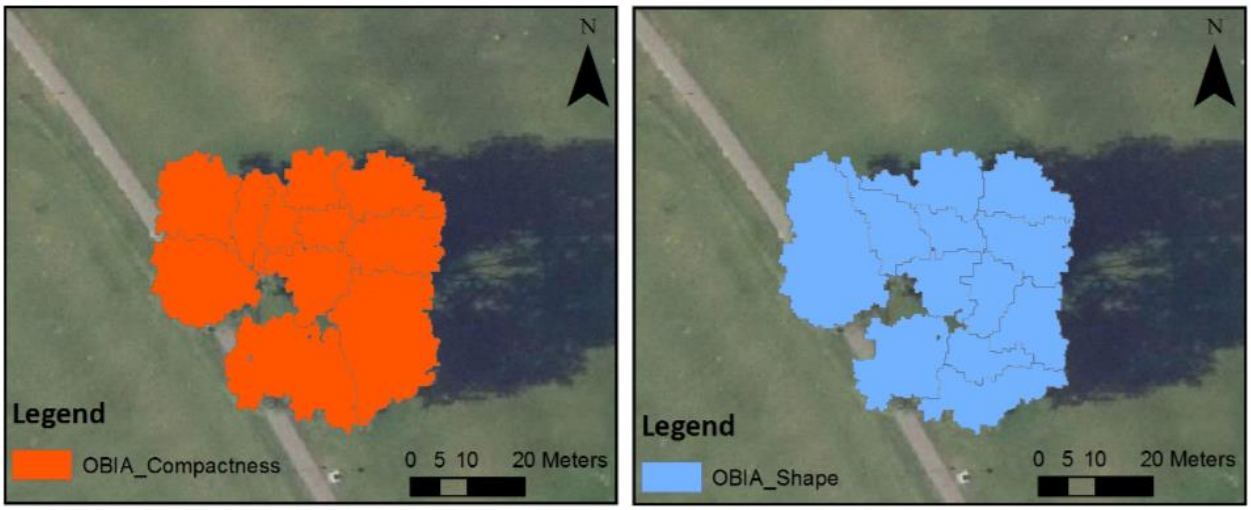

Figure 32: Visual comparison between results of ScaleParameter variant and Shape variant

The differences for the individual trees in the group are clearly distinguishable, however if the areas in the groups are combined, the images look very similar. From the similarity results this effect is less clear, because for all tree composition types, the results are quite close.

6.2.3 Hybrid method

For the newly created hybrid method only one variant was executed, which is based on the best practices of the DSM- and OBIA-methods. The best practices are decided by comparing the similarity results of all variants that were executed in this study. The results of both methods show that the best results were obtained when using the AHN3 with a resolution of 25cm as input. Therefore, the same input data was used in the hybrid method as well. Furthermore, the highest average crown similarity percentage relative to the validation dataset is for both DSM- and OBIA-methods in most cases the variant that uses the default input parameters. For the hybrid method, the default filter parameters were used from the DSM-method and the default multiresolution segmentation parameter settings were used from the OBIA-method. The crown growth delineation algorithm from the OBIA-method was very suitable for delineating the individual tree crowns resulting in the highest overall count similarity percentage.

This new, hybrid method is using the multiresolution segmentation technique used in the OBIA-method, because the growth algorithm uses the different segments as input. The DSM-method is included in this hybrid method by using the filters before executing the segmentation. By applying these filters beforehand, the segmentation is more accurate, because the overall homogeneity of the CIR image will increase. This leads to a larger relative contrast between pixels that are within the tree crowns, because most pixels outside the crown areas have been filtered out using the default DSM-filter as shown in Figure 14. When looking at the results of the multiresolution segmentation in Figure 27, it shows an interesting pattern of segments that are created over the filtered area. In these locations, the

homogeneity of the pixels is the same, because all pixels have no data. Therefore, the scale parameter threshold should be the only influencing factor that determines the maximum size of these segments. It is not clear what causes the different segments in these areas to show differences in shape and size.

The final research objective in this study is to develop a new, improved method. The results of the hybrid method are compared to the variants of the DSM- and OBIA-method that use the AHN3 at a resolution of 25cm as input and the default model parameters. The results of these variants are the closest to the validation dataset and the same input is used for the combined method. For the single trees, the hybrid method has a 100% count similarity and has the highest area similarity percentage of all methods, resulting in the highest average similarity percentage as well. When comparing the rows, the hybrid method has a relative low count similarity, but has the highest area similarity percentage when crowns are considered as individuals, as well as when crown areas of trees in rows are combined.

Finally, for the groups of trees the hybrid method has the lowest count similarity percentage and the lowest area similarity percentage. Overall, the results of the hybrid method have the best crown area similarity percentage compared to the DSM- and OBIA-methods, but the worst count similarity percentage. Therefore, the combined method is not regarded as a clear overall improvement in general. It will depend on the goal of the user, whether the combined method is more suitable for identifying tree crowns. When for example the goal is to estimate the root system area of trees, the crown area is an important indicator, so the combined method will be an improvement (Verhagen, 2015). If the goal is to estimate the number of trees in an area, the combined method is less suitable than the DSM- or OBIA-method.

6.2.4 Boombasis

It is interesting to see how the hybrid method compares to a method that is currently used in the Netherlands for tree identification. Therefore, the Boombasis is compared to the validation dataset in Den Haag as well. This makes it possible to determine how well each method performs compared to the most up-to-date Boombasis model as developed by NEO (Wigger Tims, personal communication, March 7, 2017). The Boombasis method uses the AHN3, combined with high resolution aerial images taken in the summer of 2014 (Wigger Tims, personal communication, March 7, 2017). NEO has access to high-resolution aerial images that are taken each year, therefore the results of the Boombasis are expected to be close to the validation dataset.

The version of the Boombasis that is used for the comparison is currently the most up-to-date method used in practice in the Netherlands (Wigger Tims, personal communication, March 7, 2017). The results from the Boombasis dataset are presented for all tree composition types in one table, similar to the results from the combined method.

Table 13: Results of the Boombasis method

Boombasis	Count similarity	Area similarity	Average similarity
Single trees	100.0%	93.8%	96.9%
Rows of trees individual	85.0%	80.4%	82.7%
Rows of trees total	85.0%	96.1%	90.5%
Groups of trees	54.5%	92.2%	73.4%

The results from the Boombasis in Table 13 show that the count similarity of the groups of trees is very low, with only 54.5%, which is the lowest similarity percentage of all variants tested. On the other hand, the area similarities are overall relatively high. Especially the results for both the tree crowns in rows as individuals, as for the crowns in rows combined, are the closest to the validation dataset of all methods. The area similarities to the validation dataset of the single trees and the groups of trees are over 90% as well, which is relatively high compared to most variants in the other methods. The comparison of the results from the tested methods to the results of the final Boombasis is interesting, because it shows that in some cases, for example when identifying the number of individual trees, the hybrid method would be more suitable to use. This means that for some studies, using the hybrid method will realize improvement of the results in practice.

6.2.5 Validation

Next to the tree crown identification methods that are executed in this study, the validation method that was used to compare the results has some limitations that need to be discussed as well. Validation of the individual tree crown areas is necessary to compare the results of the methods to the situation in reality (Meijer et al., 2015, p. 39). Therefore, it is important that the trees that are used for validation are a good representation of reality and ideally it would be a 100% match. That way all deviations from the validation dataset can be attributed to the methods. However, in this study no reliable validation dataset was available beforehand. Therefore, the validation was done by manually delineating the trees based on visually identifying the individual tree crowns on an aerial image with a high resolution of 5 cm. Manual delineation is never 100% accurate, because it relies on the identification interpretation of a human. If multiple people were to delineate single tree manually, it would probably never result in the exact same crown more than once. Especially for groups of trees it is difficult to see the intertwined crowns and to determine where one branch ends and another begins. Furthermore, because the crowns are intertwined, the crown areas often overlap vertically. It is not possible to visually identify this based on the aerial images. Therefore, in this study the validation crowns are not intertwined and are delineated based on a shared border. All tree identification methods are unable to identify overlap between crowns, so the deviations to the validation dataset because of overlap would have been present in all methods if overlap would have been included.

Besides the possible visual interpretation errors, another issue with the validation is the temporal difference between the input datasets and the validation dataset. Ideally, all data that was used would have been acquired on the same day as the validation data. However, for all datasets the exact date is unknown and only the years are available. The AHN2 is from 2008, The AHN3 is from 2014, the only available CIR ortho image is from 2016 and the validation data is either from 2013 or 2015. Therefore, it is possible that some deviations are caused by the temporal differences in tree crowns, rather than as a result of the different identification methods. Especially the variants of the DSM- and OBIA method that use the AHN2 as input will have shown larger deviations than if they would have been compared to a validation dataset from 2008, using a CIR ortho image from 2008 as well. Therefore, it is difficult to say if the poor results from the variants that use the AHN2 datasets are caused by using the AHN2, or by the temporal differences between the AHN2 and the validation data.

6.3 Recommendations

The final chapter of this thesis are the recommendations, based on the results and conclusions. The first recommendation is to use the hybrid method or default OBIA-method for identifying tree crown areas. If the count of the crown areas is important, the default OBIA method is most suitable. For all methods, input data with a horizontal resolution of 25cm will have better results than when using a resolution of 50cm. One limitation of this study is that the different input datasets are not from the same year. Therefore, the second recommendation is to use a CIR aerial image from the same year and season as the elevation model. Using the AHN3 as input is suitable for identifying trees and is available as open data. However, a downside of using AHN data is that it is not frequently updated, which makes it unsuitable for yearly monitoring applications. Furthermore, the AHN3 dataset is still incomplete and not available in the entire Netherlands. When it is finished, there can be a five-year difference between the periods of data acquirement (Actueel Hoogtebestand Nederland, n.d.).

Next to the recommendations for potential users of tree crown identification methods, this chapter aims to suggest improvements for future research on comparing the identification methods. The first step in improving the comparison method would be to compare more model parameters. Based on this study, for both the DSM- as the OBIA-method the default parameters were the closest to the validation dataset. However, if more possible parameter settings were tested, this might have been not the case. A first suggestion for future research is to write a script that automates the methods and compares the results of the more different model parameters to determine the best settings. This could optimize the method, resulting in higher similarity percentages.

Another way to improve this study is to compare the different methods to a more reliable validation dataset from the same period as the input datasets. In this study, the methods were compared in an urban environment and park area. However, it is not tested in different environments, like forests or tree nurseries. Comparing the methods in a tree nursery could be interesting for monitoring purposes and nurseries could provide validation data as well. Another improvement to the comparison could be to add more variables. In this study only the count of the individual tree crowns and their area are calculated. More research is needed to develop a method that can identify the position of

tree stems from the pointcloud data. This will help for applications such as identifying tree ownership or better estimations of tree root systems.

For further research on tree crown identification it will be interesting to compare more possible methods. Especially for yearly monitoring purposes the use of the AHN is not suitable. Both the DSM- and OBIA-method use the AHN data as input, but it might be possible to identify individual tree crowns without elevation data. By using the stem positions of trees instead of the peaks to separate the individual trees the AHN data might not be necessary. However, no standardized method is currently used in the Netherlands for identifying the stem positions and not all green space managers provide this data (Verhaar, 2016). This option is therefore not suitable for a standardized method of the entire Netherlands, but it will be an interesting method for managers who do have data on stem positions and want to monitor their tree crown areas more often than possible using the AHN. Monitoring tree crowns an annual or seasonal basis requires more frequently acquired input data, such as aerial or satellite imagery. As concluded in this thesis, the 25cm input AHN data is more suitable for identifying trees compared to the 50cm input AHN data. Furthermore, it will be interesting to see how the multiresolution segmentation technique performs when no pointcloud data is used as input. More research is needed to determine whether commercially, or even freely, available satellite images are suitable for identifying and monitoring individual tree crowns.

Literature

Actueel Hoogtebestand Nederland, (n.d.). *Inwinjaren AHN2 & AHN3*. Consulted on April 26th 2017, from: http://www.ahn.nl/common-nlm/inwinjaren-ahn2--ahn3.html

Alonzo, M., Bookhagen, B. & Roberts, D.A., (2014). *Urban tree species mapping using hyperspectral and lidar data fusion*. Remote sensing of Environment. Volume 148, Pages 70-83.

Antonarakis, A.S., Richards, K.S. & Brasington, J., (2008). *Object-based land cover classification using airborne LiDAR*. Remote Sensing of Environment. Volume 112, Issue 6, 16 June 2008, Pages 2988-2998.

Boombasis. (n.d.). *Boombasis beschrijving.* Unpublished document.

Boomregister., (2016). *Productbeschrijving*. Consulted on October 27th 2016, from: http://boomregister.nl/productbeschrijving-2015/.

Brandtberg, T. & Walter, F., (1998). *Automated delineation of individual tree crowns in high spatial resolution aerial images by multiple-scale analysis*. Machine Vision and Applications. Volume 11, Pages 64-73.

Van den Brink, L., Van Eekelen, H. & Reuvers, M., (2013). *Basisregistratie grootschalige topografie Gegevenscatalogus IMGeo 2.1.1*., Ministerie van Infrastructuur en Milieu & Geonovum.

Darwish, A., Leukert, K. & Reinhardt, W. (2003). *Image segmentation for the purpose of object-based classification*. In: Geoscience and Remote Sensing Symposium. IGARSS '032003 IEEE International (3) (2003), Pages 2039-2041.

Davids, L., (2013). *Using LiDAR in combination with aerial photographs to model and discriminate green small landscape elements*. Consulted on February 9th, from: https://dspace.library.uu.nl/handle/1874/281279.

Definiens., (2009). *Working with LiDAR *.las fils. New OBIA dimensions*. Definiens AG, München, Germany.

Dezsö, B., Fekete, I., Gera, D., Giachetta, R. & László, I., (2012). *Object-Based Image Analysis in Remote Sensing Applications Using Various Segmentation Techniques*. Annales Univ. Sci. Budapest., Sect. Comp. Volume 37, Pages 103-120.

Fernandez-Diaz, J. C. (2011). *Lifting the Canopy Veil - Airborne LiDAR for Archeology of Forested Areas*. Imaging Notes, 26(2).

Guo, L., Chehata, N., Mallet, C. & Buikir, S., (2011). *Relevance of airborne lidar and multispectral image data for urban scene classification using Random Forests*. ISPRS Journal of Photogrammetry and Remote Sensing. Volume 66, Issue 1, January 2011, Pages 56-66.

Haara, A. & Haarala, M., (2002). *Tree Species Classification using Semi-automatic Delineation of Trees on Aerial Images*. Scandinavian Journal of Forest Research 17:6, Pages 556-565.

Hay, G.J. & Castilla, G., (2006). *Object-Based Image Analysis: Strengths, Weaknesses, Opportunities and Threats (SWOT)*. Foothills Facility for Remote Sensing and GIScience, Department of Geography, University of Calgary, Earth Sciences, Calgary, AB, Canada.

Van Herzele, A. & Wiedemann, T., (2003). *A monitoring tool for the provision of accessible and atractive urban green spaces*. Landscape and Urban Planning 63, Pages 109-126.

Jing, L., Hu, B., Noland, T. & Li, J., (2012). *An individual tree crown delineation method based on multi-scale segmentation of imagery*. ISPRS Journal of Photogrammetry and Remote Sensing. Volume 70, Pages 88-98.

Ke, Y. & Quackenbush, L.J., (2017). *A review of methods for automatic individual tree-crown detection and delineation from passive remote sensing*. International Journal of Remote Sensing. Volume 32, No. 17, Pages 4725-4747

Landmap., (n.d.). *Contrast Filter Segmentation*. C Consulted on April 28th 2017, from: http://learningzone.rspsoc.org.uk/index.php/Learning-Materials/Object-oriented-Classification/2.10.-Contrast-Filter-Segmentation.

Leigh, C.L., Kidner, D.B. & Thomas, M.C., (2009). The Use of LiDAR in Digital Surface Modelling: Issues and Errors. Transactions in GIS. Volume 13, Issue 4, Pages 345-361.

Meijer, M., Rip, F., Van Benthem, R., Clement, J. & Van der Sande, C., (2015). *Boomkronen afleiden uit het Actueel Hoogtebestand Nederland*. Alterra Wageningen UR. Wageningen, November 2015.

Middleton, M., Schnur, T., Soronen-Ward, P. & Hyvönen, E., (2015). *Geological lineament interpretation using the object-based image analysis approach: Results of semi-automated analyses versus visual interpretation.* Geological Survey of Finland, Special Paper 57. Pages 135-154.

Mills, S., & McLeod, P., (2013). *Global seamline networks for orthomosaic generation via local search*. ISPRS Journal of Photogrammetry and Remote Sensing. Volume 75, Pages 101-111.

Nationaal Georegister., (2017). Consulted on April 26th 2017, from: http://nationaalgeoregister.nl/geonetwork/srv/dut/catalog.search#/metadata/afe2131c-8ffc-4975-a171-654745a320a4?tab=general.

Nijhuis, S., (2013). *Nieuw gereedschap. Digitale media in de landschapsarchitectuur*. In Vlug, J., Noortman, A., Aben, R., Ter Mull, B. & Hendriks, M., 2013. De noodzaak van ontwerpen.

Priestnall, G., Jaafar, J. & Duncan, A., (2000). *Extracting urban features from LiDAR digital surface models*. Computers, Environment and Urban Systems. Volume 24, Issue 2, Pages 65-78.

rapidlasso GmbH, (n.d.). *LAStools README*. Consulted on October 5th 2017, from: https://rapidlasso.com/lastools/

Swart, L., (2010). *How the Up-to-date Height Model of the Netherlands (AHN) became a massive point data cloud*. In Van Oosterom, P., Vosselman, M., Van Dijk, A. & Uitentuis, M., 2010. Management of massive point could data: wet and dry. NCG KNAW, Pages 17-32.

Verhaar, J., (2016). *Boomregister kent alle bomen*. In GIS magazine Juli/Augustus 2016 – Jaargang 14, Page 29.

Verhagen, J., (2015). *Aanbieding Boombasis 2015*. Consulted on September 15th 2016, from: http://boomregister.nl/aanbieding-boombasis/.

Wageningen University., (2014). *Object-based image analysis*. Consulted on April 28th 2017, from: http://scomp5063.wur.nl/courses/grs20306/course/Schedule/Object-based%20classification%202014.pdf.

Wang, L., (2008). *A Multi-scale Approach for Delineating Individual Tree Crowns with Very High resolution Imagery*. Photogrammetric Engineering & Remote Sensing. Volume 76, No. 4, April 2010, Pages 371-378.

White, D. & Kiester, A. R., (2008). *Topology Matters: Network topology affects outcomes from community ecology neutral models*. Computers, Environment and Urban Systems. Volume 32, No. 2, March 2008, Pages 165 – 171.

Yan, G., (2003). *Pixel based and oriented image analysis for coal fire research.* International Institute for Geo-Information Science and Earth Observation Enschede, The Netherlands.

Van der Zon, N., (2013*). Kwaliteitsdocument AHN2*. Consulted on September 21st, 2016, from http://www.ahn.nl/binaries/content/assets/hwh---ahn/common/wat+is+het+ahn/kwaliteitsdocument_ahn_versie_1_3.pdf

Appendix I: Overview of materials

Table of Content of the ZIP file and DVD that accompanies this thesis report.

- **Report**
  - Thesis report (in PDF & Word)
- **Presentations**
  - Midterm presentation (in PowerPoint)
  - Final presentation (in PowerPoint)
- **Input datasets**
  - AHN 2& 3 pointclouds and rasters (link to download page due to size)
  - Beeldmateriaal aerial raster images (link to WMTS due to size)
  - BAG data as polygons (in .shp)
- **Validation datasets**
  - Den Haag validation aerial raster images (in .tif)
  - Den Haag stem position points (in .shp)
- **Additional datasets**
  - Boombasis polygons (in .shp)
- **Output datasets**
  - Identified polygons (in .shp)
- **Literature**
  - Used Literature (in PDF)

Appendix II: All results

In this appendix, the results of all parameter variables of all methods are shown. The first table is the validation dataset, in which trees or tree groups have an ID. In the other tables, the count and area are compared to the trees in the validation dataset with the same ID. The rows have both the instances where the trees are considered as individuals and the totals at the top where the individuals are summed up.

Validation Set			
	TreeID	*Count*	*Area*
	ID	*n*	*m2*
Single	ST1	1	251.55
	ST2	1	99.81
	ST3	1	146.38
	ST4	1	106.86
	ST5	1	24.5
	ST6	1	103.71
	ST7	1	63.17
Rows	RT1	5	897.76
	RT1_A	1	175.9
	RT1_B	1	274.02
	RT1_C	1	77.19
	RT1_D	1	143.4
	RT1_E	1	227.25
	RT2	6	442.06
	RT2_A	1	89.71
	RT2_B	1	63.38
	RT2_C	1	77.64
	RT2_D	1	60.97
	RT2_E	1	79.14
	RT2_F	1	71.22
	RT3	6	547.54
	RT3_A	1	107.66
	RT3_B	1	97.11
	RT3_C	1	92.24
	RT3_D	1	66.43
	RT3_E	1	67.64
	RT3_F	1	116.46
Groups	GT1	3	999.63
	GT2	3	139.09
	GT3	6	372.53
	GT5	6	341.29

Boombasis					
	TreeID	*Count*	*Area*	*Count difference*	*Area difference*
	ID	*n*	*m2*	*n*	*m2*
Single trees	ST1	1	239	0	12.55
	ST2	1	87.5	0	12.31
	ST3	1	147.75	0	1.37
	ST4	1	96	0	10.86
	ST5	1	20.5	0	4
	ST6	1	109.5	0	5.79
	ST7	1	57.75	0	5.42
Rows of trees	RT1	8	882.5	3	15.26
	RT1_A	2	137.25	1	38.65
	RT1_B	1	187.75	0	86.27
	RT1_C	3	192.75	2	115.56
	RT1_D	1	184.25	0	40.85
	RT1_E	1	180.5	0	46.75
	RT2	6	478.5	0	36.44
	RT2_A	1	98.25	0	8.54
	RT2_B	1	68	0	4.62
	RT2_C	1	75.75	0	1.89
	RT2_D	1	85.75	0	24.78
	RT2_E	1	92.25	0	13.11
	RT2_F	1	58.5	0	12.72
	RT3	6	573.25	0	25.71
	RT3_A	1	137.75	0	30.09
	RT3_B	1	100.25	0	3.14
	RT3_C	1	90.25	0	1.99
	RT3_D	1	60.5	0	5.93
	RT3_E	1	80.75	0	13.11
	RT3_F	1	103.75	0	12.71
Groups of trees	GT1	10	901.25	7	98.38
	GT2	3	136.5	0	2.59
	GT3	2	400.25	4	27.72
	GT5	2	313.5	4	27.79

DSM Default					
	TreeID	*Count*	*Area*	*Count difference*	*Area difference*
	ID	*n*	*m2*	*n*	*m2*
Single trees	ST1	2	189.75	1	61.8
	ST2	1	75	0	24.81
	ST3	1	108.75	0	37.63
	ST4	1	39.75	0	67.11
	ST5	1	19	0	5.5
	ST6	1	181	0	77.29
	ST7	1	30.25	0	32.92
Rows of trees	RT1	5	645.5	0	252.26
	RT1_A	1	123.25	0	52.65
	RT1_B	1	132.5	0	141.52
	RT1_C	1	106.75	0	29.56
	RT1_D	1	127.75	0	15.65
	RT1_E	1	155.25	0	72
	RT2	6	393	0	49.06
	RT2_A	1	74.5	0	15.21
	RT2_B	1	52	0	11.38
	RT2_C	1	70.75	0	6.89
	RT2_D	1	49.75	0	11.22
	RT2_E	1	72	0	7.14
	RT2_F	1	74	0	2.78
	RT3	6	364.25	0	183.29
	RT3_A	1	63	0	44.66
	RT3_B	1	59.5	0	37.61
	RT3_C	1	62.75	0	29.49
	RT3_D	1	44	0	22.43
	RT3_E	1	61.5	0	6.14
	RT3_F	1	73.5	0	42.96
Groups of trees	GT1	3	733.25	0	266.38
	GT2	3	80.5	0	58.59
	GT3	3	292.75	3	79.78
	GT5	3	230.5	3	110.79

DSM AHN3					
	TreeID	*Count*	*Area*	*Count difference*	*Area difference*
	ID	*n*	*m2*	*n*	*m2*
Single trees	ST1	2	218.5	1	33.05
	ST2	1	99	0	0.81
	ST3	1	127.25	0	19.13
	ST4	1	84.75	0	22.11
	ST5	1	22.75	0	1.75
	ST6	1	95.25	0	8.46
	ST7	1	62	0	1.17
Rows of trees	RT1	6	688	1	209.76
	RT1_A	2	97	1	78.9
	RT1_B	1	187.5	0	86.52
	RT1_C	1	95.75	0	18.56
	RT1_D	1	135.75	0	7.65
	RT1_E	1	172	0	55.25
	RT2	6	441.75	0	0.31
	RT2_A	1	85	0	4.71
	RT2_B	1	59.75	0	3.63
	RT2_C	1	72.25	0	5.39
	RT2_D	1	66.5	0	5.53
	RT2_E	1	87.75	0	8.61
	RT2_F	1	70.5	0	0.72
	RT3	7	718.75	1	171.21
	RT3_A	1	100.25	0	7.41
	RT3_B	2	101.75	1	4.64
	RT3_C	1	107.5	0	15.26
	RT3_D	1	143.25	0	76.82
	RT3_E	1	91.5	0	23.86
	RT3_F	1	174.5	0	58.04
Groups of trees	GT1	3	907.5	0	92.13
	GT2	3	203.75	0	64.66
	GT3	4	399.25	2	26.72
	GT5	3	227	3	114.29

DSM AHN3 25cm					
	TreeID	*Count*	*Area*	*Count difference*	*Area difference*
	ID	*n*	*m2*	*n*	*m2*
Single trees	ST1	2	202.75	1	48.8
	ST2	1	95.25	0	4.56
	ST3	1	121.5	0	24.88
	ST4	1	101.5	0	5.36
	ST5	1	20.5	0	4
	ST6	1	105.75	0	2.04
	ST7	1	63.5	0	0.33
Rows of trees	RT1	5	762.5	0	135.26
	RT1_A	1	167.25	0	8.65
	RT1_B	1	149.5	0	124.52
	RT1_C	1	139.25	0	62.06
	RT1_D	1	128.25	0	15.15
	RT1_E	1	178.25	0	49
	RT2	6	412.25	0	29.81
	RT2_A	1	80.5	0	9.21
	RT2_B	1	55.5	0	7.88
	RT2_C	1	68.5	0	9.14
	RT2_D	1	57.5	0	3.47
	RT2_E	1	87	0	7.86
	RT2_F	1	63.25	0	7.97
	RT3	6	504	0	43.54
	RT3_A	1	25.5	0	82.16
	RT3_B	1	102.5	0	5.39
	RT3_C	1	91.5	0	0.74
	RT3_D	1	100.5	0	34.07
	RT3_E	1	155.5	0	87.86
	RT3_F	1	28.5	0	87.96
Groups of trees	GT1	3	941	0	58.63
	GT2	3	169.25	0	30.16
	GT3	2	406	4	33.47
	GT5	4	273	2	68.29

DSM AHN3 large neighborhood					
	TreeID	*Count*	*Area*	*Count difference*	*Area difference*
	ID	*n*	*m2*	*n*	*m2*
Single trees	ST1	2	202.75	1	48.8
	ST2	1	95.25	0	4.56
	ST3	1	121.5	0	24.88
	ST4	1	101.5	0	5.36
	ST5	1	20.5	0	4
	ST6	1	105.75	0	2.04
	ST7	1	63.5	0	0.33
Rows of trees	RT1	5	762.5	0	135.26
	RT1_A	1	167.25	0	8.65
	RT1_B	1	149.5	0	124.52
	RT1_C	1	139.25	0	62.06
	RT1_D	1	128.25	0	15.15
	RT1_E	1	178.25	0	49
	RT2	6	412.25	0	29.81
	RT2_A	1	80.5	0	9.21
	RT2_B	1	55.5	0	7.88
	RT2_C	1	68.5	0	9.14
	RT2_D	1	57.5	0	3.47
	RT2_E	1	87	0	7.86
	RT2_F	1	63.25	0	7.97
	RT3	6	967	0	419.46
	RT3_A	1	118.75	0	11.09
	RT3_B	1	173.25	0	76.14
	RT3_C	1	229.5	0	137.26
	RT3_D	1	165.5	0	99.07
	RT3_E	1	100.5	0	32.86
	RT3_F	1	179.5	0	63.04
Groups of trees	GT1	2	940.25	1	59.38
	GT2	3	199.75	0	60.66
	GT3	2	406	4	33.47
	GT5	3	271	3	70.29

DSM AHN3 small neighborhood					
	TreeID	*Count*	*Area*	*Count difference*	*Area difference*
	ID	*n*	*m2*	*n*	*m2*
Single trees	ST1	4	201.5	3	50.05
	ST2	1	95	0	4.81
	ST3	1	121.5	0	24.88
	ST4	2	100.5	1	6.36
	ST5	1	20.5	0	4
	ST6	2	105.25	1	1.54
	ST7	1	63.5	0	0.33
Rows of trees	RT1	5	699.25	0	198.51
	RT1_A	1	166	0	9.9
	RT1_B	1	145	0	129.02
	RT1_C	1	81.75	0	4.56
	RT1_D	1	128.25	0	15.15
	RT1_E	1	178.25	0	49
	RT2	6	412	0	30.06
	RT2_A	1	80.5	0	9.21
	RT2_B	1	55.5	0	7.88
	RT2_C	1	68.5	0	9.14
	RT2_D	1	57.5	0	3.47
	RT2_E	1	87	0	7.86
	RT2_F	1	63	0	8.22
	RT3	6	656.5	0	108.96
	RT3_A	1	102.5	0	5.16
	RT3_B	1	91.5	0	5.61
	RT3_C	1	124.75	0	32.51
	RT3_D	1	164.75	0	98.32
	RT3_E	1	100.5	0	32.86
	RT3_F	1	72.5	0	43.96
Groups of trees	GT1	5	939.5	2	60.13
	GT2	3	103	0	36.09
	GT3	4	405.5	2	32.97
	GT5	4	271.75	2	69.54

DSM NDVI					
	TreeID	*Count*	*Area*	*Count difference*	*Area difference*
	ID	*n*	*m2*	*n*	*m2*
Single trees	ST1	1	152	0	99.55
	ST2	1	94	0	5.81
	ST3	1	46.75	0	99.63
	ST4	1	96.75	0	10.11
	ST5	1	17.25	0	7.25
	ST6	1	41.25	0	62.46
	ST7	1	63.5	0	0.33
Rows of trees	RT1	5	504.5	0	393.26
	RT1_A	1	114.5	0	61.4
	RT1_B	1	83.5	0	190.52
	RT1_C	1	118.25	0	41.06
	RT1_D	1	62	0	81.4
	RT1_E	1	126.25	0	101
	RT2	6	365.5	0	76.56
	RT2_A	1	80.5	0	9.21
	RT2_B	1	46.5	0	16.88
	RT2_C	1	67.25	0	10.39
	RT2_D	1	35.5	0	25.47
	RT2_E	1	75	0	4.14
	RT2_F	1	60.75	0	10.47
	RT3	8	544	2	3.54
	RT3_A	1	74.75	0	32.91
	RT3_B	1	88.5	0	8.61
	RT3_C	1	112.25	0	20.01
	RT3_D	2	146	1	79.57
	RT3_E	2	64	1	3.64
	RT3_F	1	58.5	0	57.96
Groups of trees	GT1	3	940.25	0	59.38
	GT2	3	169	0	29.91
	GT3	2	395.5	4	22.97
	GT5	3	193	3	148.29

DSM Roughness					
	TreeID	*Count*	*Area*	*Count difference*	*Area difference*
	ID	*n*	*m2*	*n*	*m2*
Single trees	ST1	2	201	1	50.55
	ST2	1	77.25	0	22.56
	ST3	1	119.5	0	26.88
	ST4	1	94	0	12.86
	ST5	1	15	0	9.5
	ST6	2	97.5	1	6.21
	ST7	1	60.5	0	2.67
Rows of trees	RT1	5	744.5	0	153.26
	RT1_A	1	165.5	0	10.4
	RT1_B	1	142.75	0	131.27
	RT1_C	1	136.5	0	59.31
	RT1_D	1	127	0	16.4
	RT1_E	1	172.75	0	54.5
	RT2	6	406.25	0	35.81
	RT2_A	1	79	0	10.71
	RT2_B	1	55	0	8.38
	RT2_C	1	68.25	0	9.39
	RT2_D	1	56.25	0	4.72
	RT2_E	1	85.25	0	6.11
	RT2_F	1	62.5	0	8.72
	RT3	6	767.75	0	220.21
	RT3_A	1	100.5	0	7.16
	RT3_B	1	84	0	13.11
	RT3_C	1	123.5	0	31.26
	RT3_D	1	309.25	0	242.82
	RT3_E	1	93.75	0	26.11
	RT3_F	1	56.75	0	59.71
Groups of trees	GT1	3	922.5	0	77.13
	GT2	3	148.5	0	9.41
	GT3	2	392	4	19.47
	GT5	4	232	2	109.29

OBIA Default					
	TreeID	*Count*	*Area*	*Count difference*	*Area difference*
	ID	*n*	*m2*	*n*	*m2*
Single trees	ST1	1	226	0	25.55
	ST2	1	100.06	0	0.25
	ST3	1	130.31	0	16.07
	ST4	1	86.25	0	20.61
	ST5	1	22.69	0	1.81
	ST6	1	108.38	0	4.67
	ST7	1	59	0	4.17
Rows of trees	RT1	5	944.76	0	47
	RT1_A	1	273.31	0	97.41
	RT1_B	1	114.63	0	159.39
	RT1_C	1	204.69	0	127.5
	RT1_D	1	182.94	0	39.54
	RT1_E	1	169.19	0	58.06
	RT2	6	432.57	0	9.49
	RT2_A	1	71.94	0	17.77
	RT2_B	1	62.5	0	0.88
	RT2_C	1	71.63	0	6.01
	RT2_D	1	71.5	0	10.53
	RT2_E	1	88.75	0	9.61
	RT2_F	1	66.25	0	4.97
	RT3	6	503.14	0	44.4
	RT3_A	1	80.63	0	27.03
	RT3_B	1	70.44	0	26.67
	RT3_C	1	113.38	0	21.14
	RT3_D	1	100.25	0	33.82
	RT3_E	1	81.44	0	13.8
	RT3_F	1	57	0	59.46
Groups of trees	GT1	4	928.89	1	70.74
	GT2	3	166.07	0	26.98
	GT3	3	408.94	3	36.41
	GT5	4	276.82	2	64.47

OBIA 50cm					
	TreeID	*Count*	*Area*	*Count difference*	*Area difference*
	ID	*n*	*m2*	*n*	*m2*
Single trees	ST1	1	279.5	0	27.95
	ST2	1	113.75	0	13.94
	ST3	1	140.25	0	6.13
	ST4	1	114.5	0	7.64
	ST5	1	26.5	0	2
	ST6	1	131.25	0	27.54
	ST7	1	72.5	0	9.33
Rows of trees	RT1	5	977.75	0	79.99
	RT1_A	1	305.5	0	129.6
	RT1_B	1	170	0	104.02
	RT1_C	1	158.75	0	81.56
	RT1_D	1	154.25	0	10.85
	RT1_E	1	189.25	0	38
	RT2	6	510.25	0	68.19
	RT2_A	1	92.25	0	2.54
	RT2_B	1	68	0	4.62
	RT2_C	1	72.25	0	5.39
	RT2_D	1	76.75	0	15.78
	RT2_E	1	119.75	0	40.61
	RT2_F	1	81.25	0	10.03
	RT3	6	873	0	325.46
	RT3_A	1	193	0	85.34
	RT3_B	1	80.75	0	16.36
	RT3_C	1	211.75	0	119.51
	RT3_D	1	215.5	0	149.07
	RT3_E	1	98.25	0	30.61
	RT3_F	1	73.75	0	42.71
Groups of trees	GT1	4	1016.25	1	16.62
	GT2	3	121.35	0	17.74
	GT3	2	444.75	4	72.22
	GT5	3	314	3	27.29

OBIA AHN2 50cm					
	TreeID	*Count*	*Area*	*Count difference*	*Area difference*
	ID	*n*	*m2*	*n*	*m2*
Single trees	ST1	1	242.75	0	8.8
	ST2	1	89	0	10.81
	ST3	1	113.25	0	33.13
	ST4	1	64.75	0	42.11
	ST5	1	24.4	0	0.1
	ST6	1	220	0	116.29
	ST7	1	38	0	25.17
Rows of trees	RT1	5	806.25	0	91.51
	RT1_A	1	129.25	0	46.65
	RT1_B	1	255	0	19.02
	RT1_C	1	52.75	0	24.44
	RT1_D	1	194.25	0	50.85
	RT1_E	1	175	0	52.25
	RT2	2	503	4	60.94
	RT2_A	1	224.75	0	135.04
	RT2_B	0	0	1	63.38
	RT2_C	1	278.25	0	200.61
	RT2_D	0	0	1	60.97
	RT2_E	0	0	1	79.14
	RT2_F	0	0	1	71.22
	RT3	5	484	1	63.54
	RT3_A	1	86.5	0	21.16
	RT3_B	1	71.75	0	25.36
	RT3_C	1	137	0	44.76
	RT3_D	1	87.75	0	21.32
	RT3_E	1	101	0	33.36
	RT3_F	0	0	1	116.46
Groups of trees	GT1	6	887.25	3	112.38
	GT2	2	123.75	1	15.34
	GT3	4	455	2	82.47
	GT5	5	385.75	1	44.46

OBIA Weights					
	TreeID	*Count*	*Area*	*Count difference*	*Area difference*
	ID	*n*	*m2*	*n*	*m2*
Single trees	ST1	1	233.56	0	17.99
	ST2	1	96.21	0	3.6
	ST3	1	133.56	0	12.82
	ST4	1	91.88	0	14.98
	ST5	1	21.75	0	2.75
	ST6	1	110	0	6.29
	ST7	1	61.38	0	1.79
Rows of trees	RT1	5	718.62	0	179.14
	RT1_A	1	165.06	0	10.84
	RT1_B	1	160.37	0	113.65
	RT1_C	1	68.38	0	8.81
	RT1_D	1	147.5	0	4.1
	RT1_E	1	177.31	0	49.94
	RT2	5	483.15	1	41.09
	RT2_A	1	133.38	0	43.67
	RT2_B	1	49.69	0	13.69
	RT2_C	1	109.21	0	31.57
	RT2_D	0	0	1	60.97
	RT2_E	1	125.81	0	46.67
	RT2_F	1	65.06	0	6.16
	RT3	6	475.25	0	72.29
	RT3_A	1	75.38	0	32.28
	RT3_B	1	94.06	0	3.05
	RT3_C	1	84.81	0	7.43
	RT3_D	1	84.56	0	18.13
	RT3_E	1	87.25	0	19.61
	RT3_F	1	49.19	0	67.27
Groups of trees	GT1	6	936.25	3	63.38
	GT2	3	184.32	0	45.23
	GT3	3	470.76	3	98.23
	GT5	3	280.38	3	60.91

OBIA Scale Parameter					
	TreeID	*Count*	*Area*	*Count difference*	*Area difference*
	ID	*n*	*m2*	*n*	*m2*
Single trees	ST1	1	216.75	0	34.8
	ST2	1	106.75	0	6.94
	ST3	1	133.19	0	13.19
	ST4	1	92.56	0	14.3
	ST5	1	27.19	0	2.69
	ST6	1	120.25	0	16.54
	ST7	1	67.5	0	4.33
Rows of trees	RT1	5	737.18	0	160.58
	RT1_A	1	208.81	0	32.91
	RT1_B	1	144.31	0	129.71
	RT1_C	1	56.31	0	20.88
	RT1_D	1	148.81	0	5.41
	RT1_E	1	178.94	0	48.31
	RT2	7	481.45	1	39.39
	RT2_A	1	95.06	0	5.35
	RT2_B	1	60.88	0	2.5
	RT2_C	2	79.63	1	1.99
	RT2_D	1	85.69	0	24.72
	RT2_E	1	105.25	0	26.11
	RT2_F	1	54.94	0	16.28
	RT3	5	567.07	1	19.53
	RT3_A	1	116.56	0	8.9
	RT3_B	1	89.19	0	7.92
	RT3_C	1	173.38	0	81.14
	RT3_D	1	67.19	0	0.76
	RT3_E	1	120.75	0	53.11
	RT3_F	0	0	1	116.46
Groups of trees	GT1	7	938.06	4	61.57
	GT2	3	175.94	0	36.85
	GT3	6	405.33	0	32.8
	GT5	3	272.13	3	69.16

OBIA Shape					
	TreeID	*Count*	*Area*	*Count difference*	*Area difference*
	ID	*n*	*m2*	*n*	*m2*
Single trees	ST1	1	230.13	0	21.42
	ST2	1	98.63	0	1.18
	ST3	1	132.31	0	14.07
	ST4	1	95.94	0	10.92
	ST5	1	25.38	0	0.88
	ST6	1	109.5	0	5.79
	ST7	1	62	0	1.17
Rows of trees	RT1	5	778.5	0	119.26
	RT1_A	1	157.94	0	17.96
	RT1_B	1	171.75	0	102.27
	RT1_C	1	121.5	0	44.31
	RT1_D	1	151	0	7.6
	RT1_E	1	176.31	0	50.94
	RT2	5	474.75	1	32.69
	RT2_A	1	118.56	0	28.85
	RT2_B	1	81.69	0	18.31
	RT2_C	1	83.13	0	5.49
	RT2_D	0	0	1	60.97
	RT2_E	1	129.56	0	50.42
	RT2_F	1	61.81	0	9.41
	RT3	6	504.07	0	43.47
	RT3_A	1	87.94	0	19.72
	RT3_B	1	63.88	0	33.23
	RT3_C	1	113.31	0	21.07
	RT3_D	1	105.06	0	38.63
	RT3_E	1	82.19	0	14.55
	RT3_F	1	51.69	0	64.77
Groups of trees	GT1	4	935.06	1	64.57
	GT2	3	212.06	0	72.97
	GT3	1	416.25	5	43.72
	GT5	4	284	2	57.29

OBIA Compactness					
	TreeID	*Count*	*Area*	*Count difference*	*Area difference*
	ID	*n*	*m2*	*n*	*m2*
Single trees	ST1	1	223.75	0	27.8
	ST2	1	93	0	6.81
	ST3	1	132.25	0	14.13
	ST4	1	92.44	0	14.42
	ST5	1	23.38	0	1.12
	ST6	1	105.81	0	2.1
	ST7	1	60.75	0	2.42
Rows of trees	RT1	5	761.2	0	136.56
	RT1_A	1	158.88	0	17.02
	RT1_B	1	128	0	146.02
	RT1_C	1	133.75	0	56.56
	RT1_D	1	166.44	0	23.04
	RT1_E	1	174.13	0	53.12
	RT2	6	494.57	0	52.51
	RT2_A	1	89.19	0	0.52
	RT2_B	1	67.25	0	3.87
	RT2_C	1	94.94	0	17.3
	RT2_D	1	55.31	0	5.66
	RT2_E	1	121.19	0	42.05
	RT2_F	1	66.69	0	4.53
	RT3	6	477.31	0	70.23
	RT3_A	1	78.81	0	28.85
	RT3_B	1	91.44	0	5.67
	RT3_C	1	87.87	0	4.37
	RT3_D	1	89.81	0	23.38
	RT3_E	1	73.13	0	5.49
	RT3_F	1	56.25	0	60.21
Groups of trees	GT1	5	927.76	2	71.87
	GT2	3	192.63	0	53.54
	GT3	2	468.5	4	95.97
	GT5	3	287.82	3	53.47

Hybrid					
	TreeID	*Count*	*Area*	*Count difference*	*Area difference*
	ID	*n*	*m2*	*n*	*m2*
Single trees	ST1	1	236.19	0	15.36
	ST2	1	106.81	0	7
	ST3	1	142.88	0	3.5
	ST4	1	108.38	0	1.52
	ST5	1	26.75	0	2.25
	ST6	1	116.06	0	12.35
	ST7	1	69.38	0	6.21
Rows of trees	RT1	6	860.5	1	37.26
	RT1_A	1	162	0	13.9
	RT1_B	1	180.81	0	93.21
	RT1_C	1	153.81	0	76.62
	RT1_D	1	130	0	13.4
	RT1_E	2	233.88	1	6.63
	RT2	5	479.32	1	37.26
	RT2_A	1	87.63	0	2.08
	RT2_B	1	94.38	0	31
	RT2_C	1	104.5	0	26.86
	RT2_D	0	0	1	60.97
	RT2_E	1	128.56	0	49.42
	RT2_F	1	64.25	0	6.97
	RT3	7	567.75	1	20.21
	RT3_A	1	117.37	0	9.71
	RT3_B	2	97.07	1	0.04
	RT3_C	1	108.56	0	16.32
	RT3_D	1	80.94	0	14.51
	RT3_E	1	99.31	0	31.67
	RT3_F	1	64.5	0	51.96
Groups of trees	GT1	4	938.5	1	61.13
	GT2	3	233.93	0	94.84
	GT3	2	432.94	4	60.41
	GT5	4	319.12	2	22.17

Appendix III: Overview of all absolute deviations

This overview of the absolute deviations is based on the results in Appendix II. All differences with the validation set are summed up to determine how the results of the different methods perform. The results that are compared in these tables include all method variants that were used in this study. The deviation results are then coloured from green to red in each column for count and area. The similarity percentages as presented in the results chapter are based on these absolute deviations from the validation dataset.

Single trees

	Single trees count	**Single trees area**
	sum	sum
Boombasis	0.00	52.30
DSM Default	1.00	307.06
DSM AHN3	1.00	86.48
DSM AHN3 25cm	1.00	89.97
DSM AHN3 la neighbor	1.00	89.97
DSM AHN3 sm neighbor	5.00	91.97
DSM NDVI	0.00	285.14
DSM roughness	2.00	131.23
OBIA Default	0.00	73.13
OBIA CellSize	0.00	94.53
OBIA AHN2	0.00	236.41
OBIA Weights	0.00	60.22
OBIA ScaleParameter	0.00	92.79
OBIA Shape	0.00	55.43
OBIA Compactness	0.00	68.80
Hybrid	0.00	48.19

Rows

	Rows count	Rows individuals area	Rows total area
	sum	sum	sum
Boombasis	3.00	460.71	77.41
DSM Default	0.00	549.29	484.61
DSM AHN3	2.00	461.50	381.28
DSM AHN3 25cm	0.00	603.09	208.61
DSM AHN3 la neighbor	0.00	724.37	584.53
DSM AHN3 sm neighbor	0.00	471.83	337.53
DSM NDVI	2.00	754.64	473.36
DSM roughness	0.00	700.08	409.28
OBIA Default	0.00	713.59	100.89
OBIA CellSize	0.00	886.60	473.64
OBIA AHN2	5.00	1065.99	215.99
OBIA Weights	1.00	537.84	292.52
OBIA ScaleParameter	2.00	582.46	219.50
OBIA Shape	1.00	588.50	195.42
OBIA Compactness	0.00	497.66	259.30
Hybrid	3.00	505.27	94.73

Groups

	Groups count	Groups area
	sum	sum
Boombasis	15.00	156.48
DSM Default	6.00	515.54
DSM AHN3	5.00	297.80
DSM AHN3 25cm	6.00	190.55
DSM AHN3 la neighbor	8.00	223.80
DSM AHN3 sm neighbor	6.00	198.73
DSM NDVI	7.00	260.55
DSM roughness	6.00	215.30
OBIA Default	6.00	198.60
OBIA CellSize	8.00	133.87
OBIA AHN2	7.00	254.65
OBIA Weights	9.00	267.75
OBIA ScaleParameter	7.00	200.38
OBIA Shape	8.00	238.55
OBIA Compactness	9.00	274.85
Hybrid	7.00	238.55

Total

	Count	Area ind rows	Area tot rows
	sum	sum m²	sum m²
Boombasis	18	669.49	286.19
DSM Default	7	1371.89	1307.21
DSM AHN3	8	845.78	765.56
DSM AHN3 25cm	7	883.61	489.13
DSM AHN3 la neighbor	9	1038.14	898.30
DSM AHN3 sm neighbor	11	762.53	628.23
DSM NDVI	9	1300.33	1019.05
DSM roughness	8	1046.61	755.81
OBIA Default	6	985.32	372.62
OBIA CellSize	8	1115.00	702.04
OBIA AHN2	12	1557.05	707.05
OBIA Weights	10	865.81	620.49
OBIA ScaleParameter	9	875.63	512.67
OBIA Shape	9	882.48	489.40
OBIA Compactness	9	841.31	602.95
Hybrid	10	792.01	381.47